

# Heat Shock Protein Cognate 70-4 and an E3 Ubiquitin Ligase, CHIP, Mediate Plastid-Destined Precursor Degradation through the Ubiquitin-26S Proteasome System in *Arabidopsis*

Sookjin Lee,<sup>a</sup> Dong Wook Lee,<sup>a</sup> Yongjik Lee,<sup>a,b</sup> Ulrike Mayer,<sup>c</sup> York-Dieter Stierhof,<sup>c</sup> Sumin Lee,<sup>a</sup> Gerd Jürgens,<sup>c</sup> and Inhwan Hwang<sup>a,b,1</sup>

<sup>a</sup>Division of Molecular and Life Sciences, Pohang University of Science and Technology, Pohang, 790-784, Korea

<sup>b</sup>Division of Integrative Biosciences and Biotechnology, Pohang University of Science and Technology, Pohang, 790-784, Korea

<sup>c</sup>Center for Plant Molecular Biology, University of Tübingen, D-72076 Tübingen, Germany

**Plastid-targeted proteins pass through the cytosol as unfolded precursors. If proteins accumulate in the cytosol, they can form nonspecific aggregates that cause severe cellular damage. Here, we demonstrate that high levels of plastid precursors are degraded through the ubiquitin-proteasome system (UPS) in *Arabidopsis thaliana* cells. The cytosolic *heat shock protein cognate 70-4* (*Hsc70-4*) and E3 ligase *carboxy terminus of Hsc70-interacting protein* (*CHIP*) were highly induced in *plastid protein import2* plants, which had a T-DNA insertion at *Toc159* and showed an albino phenotype and a severe defect in protein import into chloroplasts. *Hsc70-4* and *CHIP* together mediated plastid precursor degradation when import-defective chloroplast-targeted reporter proteins were transiently expressed in protoplasts. *Hsc70-4* recognized specific sequence motifs in transit peptides and thereby led to precursor degradation through the UPS. *CHIP*, which interacted with *Hsc70-4*, functioned as an E3 ligase in the *Hsc70-4*-mediated protein degradation. The physiological role of *Hsc70-4* was confirmed by analyzing *Hsc70-4* RNA interference plants in an *hsc70-1* mutant background. Plants with lower *Hsc70* levels exhibited abnormal embryogenesis, resulting in defective seedlings that displayed high levels of reactive oxygen species and monoubiquitinated *Lhcb4* precursors. We propose that *Hsc70-4* and *CHIP* mediate plastid-destined precursor degradation to prevent cytosolic precursor accumulation and thereby play a critical role in embryogenesis.**

## INTRODUCTION

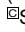
Proteins destined for the two endosymbiotic organelles (i.e., plastids and mitochondria) are targeted from the cytoplasm as unfolded precursors (Keegstra and Froehlich, 1999; Koumoto et al., 2001; Jarvis and Soll, 2002; Soll and Schleiff, 2004; Jarvis, 2008). In the cytosol, unfolded proteins have a high tendency to form cytotoxic, life-threatening, and nonspecific aggregates if they accumulate to high levels (Wickner et al., 1999; Esser et al., 2004; Meredith, 2005; Kabashi and Durham, 2006). Therefore, posttranslational targeting to endosymbiotic organelles requires that precursor levels be maintained within limits that do not result in nonspecific aggregate formation. At the same time, the cytosolic regulatory mechanism must not jeopardize the supply of sufficient amounts of proteins to the organelles.

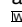
Eukaryotic cells have a protein quality control (PQC) mechanism to constantly monitor the quality of newly synthesized

proteins and preexisting proteins and to actively remove unfolded or misfolded proteins (Hartl and Hayer-Hartl, 2002; Hatakeyama and Nakayama, 2003; Esser et al., 2004). It is reported that as much as 30% of newly synthesized proteins are immediately degraded by the PQC system because of a problem in protein folding (Schubert et al., 2000). The PQC in the cytosol is achieved by two opposing processes: chaperone-assisted folding and ubiquitin/proteasome-mediated degradation. The molecular chaperones heat shock protein 70 (Hsp70) and heat shock protein cognate 70 (Hsc70), whose levels are elevated under stress conditions, assist folding of unfolded or misfolded proteins in an ATP-dependent manner (Bukau and Horwich, 1998; Dickson et al., 2000; Saibil and Ranson, 2002; Esser et al., 2004). The *Arabidopsis thaliana* genome encodes 14 Hsp70 homologs. Among them, certain isoforms are induced by abiotic and biotic stresses (Lin et al., 2001; Sung et al., 2001; Noël et al., 2007). Although their exact function is not fully elucidated in plant cells, it is likely that plant Hsc70 homologs play a role in regulating protein quality in the cytosol. In contrast with Hsc70s, the ubiquitin/proteasome system (UPS) removes unfolded or misfolded proteins through protein degradation (Esser et al., 2004). In this process, misfolded proteins are marked with polyubiquitin chain by an E2 ubiquitin-conjugating enzyme and an E3 ubiquitin ligase (Hershko et al., 2000; Cyr et al., 2002; Hatakeyama and Nakayama, 2003; Esser et al., 2004). Molecular chaperones also play a critical role in the UPS (Esser et al., 2004).

<sup>1</sup> Address correspondence to [ihhwang@postech.ac.kr](mailto:ihhwang@postech.ac.kr).

The author responsible for distribution of materials integral to the findings presented in this article in accordance with the policy described in the Instructions for Authors ([www.plantcell.org](http://www.plantcell.org)) is: Inhwan Hwang ([ihhwang@postech.ac.kr](mailto:ihhwang@postech.ac.kr)).

 Some figures in this article are displayed in color online but in black and white in the print edition.

 Online version contains Web-only data.

[www.plantcell.org/cgi/doi/10.1105/tpc.109.071548](http://www.plantcell.org/cgi/doi/10.1105/tpc.109.071548)

Plant cells may employ multiple strategies to regulate unfolded precursor levels in the cytosol. One possibility is that precursor targeting to the organelles is highly efficient. Consistent with this hypothesis, for more efficient targeting to the plastids from the cytosol, precursors often assemble into complexes with cytosolic factors, such as 14-3-3 and cytosolic Hsp70 (Jarvis and Soll, 2002; Agne and Kessler, 2009). Another possibility is that the precursor level is finely regulated either by active removal through degradation or by the downregulation of genes encoding organellar proteins if the cytosolic precursor levels exceed the import capacity. Numerous plastid protein-encoding genes are reportedly downregulated in the import-defective *plastid protein import1* (*ppi1*) and *toc132* mutants (Kubis et al., 2003, 2004), indicating that cells have a transcriptional mechanism that regulates precursor levels. However, it is not known whether cells also have a mechanism that regulates the cytosolic protein level of precursors. Such mechanisms might include removal through proteolysis, as has been observed in animal cells where unfolded protein accumulation is prevented by the UPS (Esser et al., 2004).

*Arabidopsis ppi2* mutant plants lack the import receptor Toc159 and exhibit severe defects in chloroplastic protein import (Bauer et al., 2000). However, *ppi2* plants do not accumulate high cytosolic levels of chloroplast-destined precursor proteins. Thus, we hypothesized that if plant cells have a mechanism for regulating the cytosolic precursor protein level, its components are likely increased in import-defective mutants, such as *ppi2* (Bauer et al., 2000). To test this hypothesis, we examined the fate of plastid proteins and gene activation levels in *ppi2* mutants. We found that *Hsc70-4* and the E3 ligase *carboxy terminus of Hsc70-interacting protein* (CHIP) were highly induced in *ppi2* mutant plants, where they mediated the degradation of chloroplast-targeted precursors through the UPS. We also identified *Hsc70-4* as critical in plant development.

## RESULTS

### Chloroplast Proteins in *ppi2* Mutant Plants Are Degraded by the UPS

Chloroplast-destined protein precursors do not accumulate to high levels in *ppi2* mutants, despite severely defective protein import into chloroplasts (Bauer et al., 2000). To examine the mechanism of this process, we examined the fate of these chloroplast-targeted precursors. Protein extracts from *ppi2* and wild-type plants treated with MG132, an inhibitor of 26S proteasome (Lee and Goldberg, 1998), or DMSO as a control were analyzed by protein gel blotting using an anti-Lhcb4 antibody. In previous studies, the anti-Lhcb4 antibody detected three Lhcb4 isoforms, Lhcb4.1, Lhcb4.2, and Lhcb4.3, at 29, 26, and 23 kD, respectively (Król et al., 1995; Klimek et al., 2006). Indeed, the anti-Lhcb4 antibody strongly detected bands at 29 and 23 kD, which may correspond to Lhcb4.1 and Lhcb4.3, respectively, and a weak band at 26 kD, which may correspond to Lhcb4.2. In addition, we confirmed that Lhcb4.1 migrated to the 29-kD position (see Supplemental Figure 1 online). In DMSO-treated *ppi2* plants, the amount of mature Lhcb4 was reduced to 16% of

that of wild-type plants (Figure 1A). However, despite the low levels of mature Lhcb4 proteins, there was no significant increase in their precursor levels in *ppi2* plants (Bauer et al., 2000). New protein species in the molecular mass range of 90 to 200 kD were detected in *ppi2* plants, but not in wild-type plants, by the anti-Lhcb4 antibody (Figure 1A, *ppi2* with 100  $\mu$ g of protein extracts). When *ppi2* plants were treated with MG132, the intensity of protein bands at 90 to 200 kD was markedly increased in *ppi2* plants. In addition, the intensity of the 42-kD band detected by the anti-Lhcb4 antibody was also strongly increased (indicated by \*\* in Figure 1A).

The above results raised the possibility that the new protein species were ubiquitinated Lhcb4. To test this hypothesis, *ppi2* mutant proteins were immunoprecipitated with anti-Lhcb4 antibody, and the immunoprecipitates were analyzed by protein gel blotting using anti-ubiquitin antibody. Anti-ubiquitin revealed high molecular mass proteins at  $\sim$ 90 to 200 kD and a 42-kD band from the immunoprecipitates of the anti-Lhcb4 antibody (Figure 1B). These results suggest that the high molecular mass proteins at  $\sim$ 90 to 200 kD are polyubiquitinated Lhcb4 and that the 42-kD protein species is a the monoubiquitinated Lhcb4 precursor. The calculated molecular mass of the Lhcb4 precursor was 34 kD. A negative control with rabbit serum did not precipitate any proteins that were detected with the anti-ubiquitin antibody, demonstrating the specificity of the anti-Lhcb4 antibody in the immunoprecipitation. These results suggest that unimported Lhcb4 precursors were degraded by the UPS in *ppi2* mutants.

### Numerous Genes, Including *Hsc70-4* and CHIP, Are Induced in *ppi2* Mutants

To obtain supporting evidence that chloroplast-destined proteins were degraded in *ppi2* plants, we examined whether any UPS-related genes were activated in *ppi2* plants. Initially, we randomly selected two subunits *RPN1* and *RPN5B* of 26S proteasomes and found that they were induced in *ppi2* plants by RT-PCR. Subsequently, to gain an insight into the global changes in the expression pattern of UPS-related genes as well as genes involved in protein import into chloroplasts, we performed transcriptome analysis by microarray profiling of the total RNA from *ppi2* and wild-type plants (Baldwin et al., 1999). Numerous genes were induced in *ppi2* plants (Figure 2A). However, the genes encoding the translocon components did not display any significant changes in expression level. Among the genes found to be highly induced this study, we focused on Hsp70 isoforms and E3 ligase, which may play a role in degradation of unfolded or misfolded proteins through the UPS pathway (Esser et al., 2004). One of the Hsp70 isoforms was *Hsc70-4*, a cytosolic/nuclear Hsp70 isoform that is induced by pathogen treatment (Sung et al., 2001; Noël et al., 2007).

To verify the induction of *Hsc70-4* in *ppi2* plants, we performed RT-PCR using the total RNA from wild-type and *ppi2* plants. As controls, we analyzed 12 other Hsp70s: four other Hsc70s, one BiP, two mtHsp70s, two cpHsp70s, and three additional Hsp70 isoforms with no information on their localization (named Hsp70-A, Hsp7-B, and Hsp70-C; see Supplemental Figure 2 and Supplemental Data Set 1 online) (Lin et al., 2001; Sung et al.,

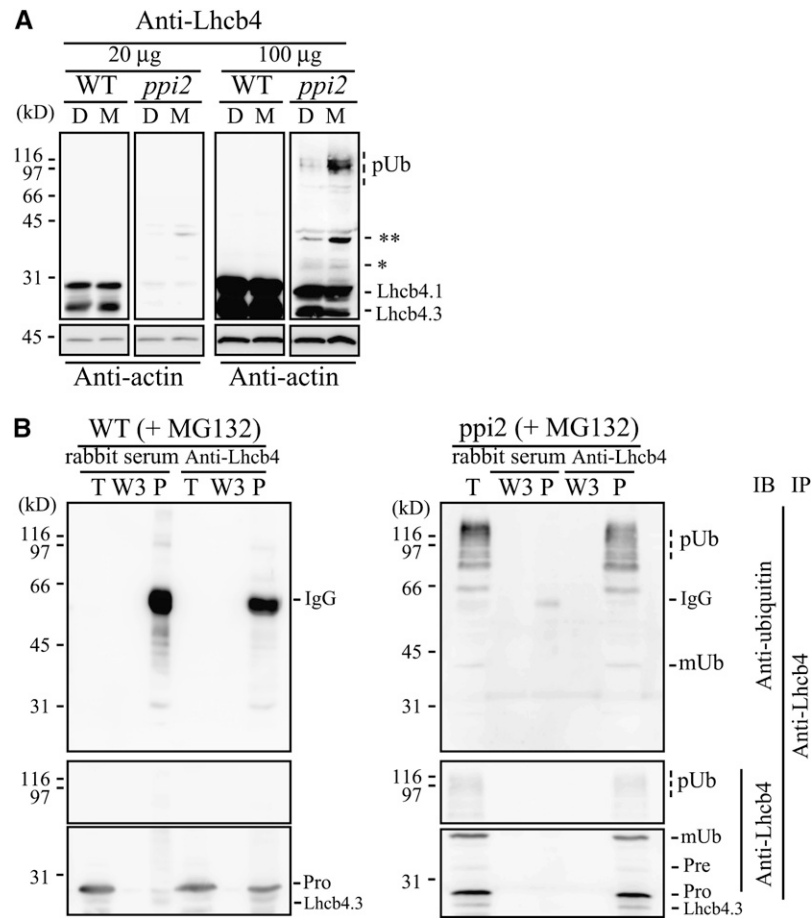


**Figure 1.** Lhcb4 Is Degraded by 26S Proteasome through Polyubiquitination in *ppi2* Mutants.

**(A)** Ubiquitination of endogenous Lhcb4 in *ppi2* plants. Protein extracts from wild-type and *ppi2* plants that had been incubated with MG132 (M) or DMSO (D) were analyzed by protein gel blotting using anti-Lhcb4 antibody. Actin was used as a loading control. Five times more *ppi2* extract than wild-type extract was loaded per gel lane. pUb, polyubiquitinated forms. Asterisks (\* and \*\*) indicate expected positions of precursor and monoubiquitinated Lhcb4.1 precursors, respectively.

**(B)** Immunoprecipitation of polyubiquitinated Lhcb4. Protein extracts from MG132-treated *ppi2* mutants were subjected to immunoprecipitation using anti-Lhcb4. As a control, immunoprecipitation was performed with unrelated rabbit serum. The immunoprecipitates were analyzed by protein gel blotting using the indicated antibodies. In the anti-Lhcb4 immunoblots, the dotted lines indicate the region that was cut out to save space. IP, immunoprecipitation; IB, immunoblot. T, 10% of total extract; W3, third washing fraction; P, precipitates; IgG, IgG heavy chain; pUb, polyubiquitinated proteins; mUb, monoubiquitinated Lhcb4.

2001). Consistent with the microarray data, *Hsc70-4* was highly induced in *ppi2* plants (Figure 2B). In addition, the four other cytosolic Hsc70 isoforms exhibited increased transcript levels, albeit to a lesser extent (Figure 2B). Previous studies have shown that Hsc70-1 mediates heat tolerance, plant development, immune response, abiotic stress response, and protein targeting to the nuclear envelope membrane (Sung and Guy, 2003; Noël et al., 2007; Brkljacic et al., 2009; Cazalé et al., 2009). Thus, each cytosolic Hsc70 isoform may have a specific function, with a degree of functional redundancy among the isoforms (Noël et al., 2007). However, *Hsp70-A*, *Hsp70-B*, *Hsp70-C*, *BiP-1*, two *mtHsp70s*, and two *cpHsp70s* exhibited no transcript level increases in *ppi2* mutants, indicating that gene induction is specific to cytosolic Hsc70 isoforms.

Since Hsc70 isoforms can be induced by heat shock (Sung et al., 2001), we examined whether the *Hsc70-4* induction in *ppi2* plants was associated with the heat shock response. RT-PCR analysis was performed using total RNA from heat-shocked *ppi2* and wild-type plants. Upon heat shock, *Hsc70s* were strongly induced in both wild-type and *ppi2* plants (Figure 2B), as were *BiP-1*, *mtHsp70-2*, *Hsp70-A*, *Hsp70-B*, and *Hsp70-C*. These results suggest that *Hsc70s* induction in *ppi2* plants is not related to heat shock but is rather either directly or indirectly related to protein import defects.

Next, we examined the underlying cause of *Hsc70-4* induction in *ppi2* mutants. T7:Toc159GM, which complements the protein import defect in *ppi2* plants when expressed in protoplasts (Figure 2C) (Lee et al., 2003), was transiently

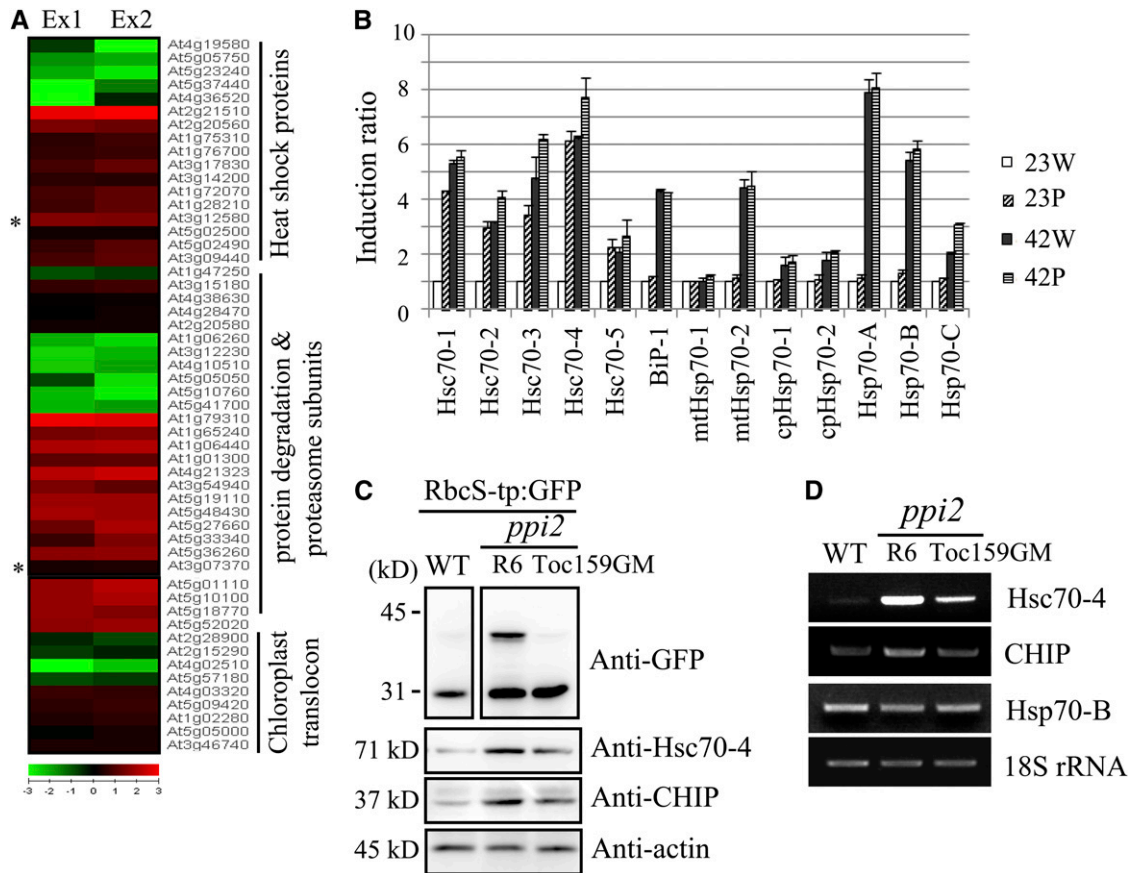


**Figure 2.** Cytosolic *Hsc70* Isoforms, in Particular *Hsc70-4* and *CHIP*, Were Highly Induced in *ppi2* Mutant Plants.

**(A)** Differential expression of 49 genes in *ppi2* mutants as determined by hierarchical clustering of microarray data. The genes involved in the heat shock response, UPS pathways, and protein import into chloroplasts were selected and analyzed for their expression patterns. Red, green, and black, upregulated, downregulated, and no change relative to the wild type, respectively; Ex1 and Ex2, two independent experiments.

**(B)** RT-PCR analysis of the transcript levels of 13 *Arabidopsis* Hsp70 homologs in *ppi2* and wild-type plants. Total RNA was prepared from *ppi2* and wild-type plants that had been treated with or without heat shock at 42°C for 30 min. RT-PCR was performed using gene-specific primers for 13 Hsp70 homologs (see Supplemental Table 1 online). The transcript levels of individual Hsp70 homologs in *ppi2* plants were compared with those in wild-type plants. The intensity of amplified PCR products after agarose gel electrophoresis was quantified. PCR was performed at the same conditions for all 13 Hsp70 homologs. Three independent experiments were performed. 23W and 23P, wild-type and *ppi2* plants at normal conditions (23°C), respectively; 42W and 42P, wild-type and *ppi2* plants treated with heat shock at 42°C for 30 min, respectively. Error bar indicates SE ( $n = 3$ ).

**(C)** *Hsc70-4* and *CHIP* protein levels in *ppi2* plants. Protein extracts from wild-type and *ppi2* plants were analyzed by protein gel blot analysis using anti-*Hsc70-4* and anti-*CHIP* antibodies. In addition, protein extracts from *ppi2* protoplasts transformed with *T7:Toc159GM* were included in the analysis. Actin levels were determined as a loading control.

**(D)** Suppression of *Hsc70-4* and *CHIP* induction by *T7:Toc159GM* in *ppi2* protoplasts. Total RNA from *ppi2* protoplasts transformed with *T7:Toc159GM*, or empty expression vector (*R6*), was used for RT-PCR analysis at the same conditions using specific primers for *Hsc70-4*, *Hsp70-B*, *CHIP*, and 18S rRNA. Total RNA from wild-type plants was included in the analysis. *ppi2* protoplasts were transformed with *RbcS-tp:GFP* together with *T7:Toc159GM* or *R6*. As a control, wild-type protoplasts were transformed with *RbcS-tp:GFP*.

expressed in *ppi2* protoplasts, and the *Hsc70-4* transcript levels were examined 12 h after transformation by RT-PCR. When *T7:Toc159GM* was transiently expressed in *ppi2* protoplasts, the *Hsc70-4* transcript levels were greatly reduced (Figure 2D). This result suggests that the accumulation of chloroplast precursors in the cytosol, rather than abnormal chloroplast development, is the underlying cause of *Hsc70-4* induction in *ppi2* plants.

Another highly induced gene in *ppi2* plants was *CHIP*, which encodes an E3 ligase. *CHIP* (*Arabidopsis* C terminus of *Hsc70-*

interacting protein) binds to ClpP4 and FtsH1 and helps regulate chloroplast protein levels (Luo et al., 2006; Shen et al., 2007a, 2007b). We examined the induction of *CHIP* in *ppi2* plants by RT-PCR. Consistent with our microarray data, semiquantitative RT-PCR confirmed the induction of *CHIP* in *ppi2* plants (Figure 2C). This induction was reduced to lower levels when *T7:Toc159GM* was transiently expressed in *ppi2* protoplasts (Figure 2C). These results, together with those presented in Figure 1, suggest that *CHIP* may play a role degradation of chloroplast-destined proteins in *ppi2* plants.

To confirm the induction of Hsc70-4 and CHIP in *ppi2* plants at the protein level, we performed protein gel blot analysis using anti-Hsc70-4 and anti-CHIP antibodies (see Supplemental Figure 3 online; Shen et al., 2007a). Total protein extracts were prepared from wild-type and *ppi2* plants. In addition, protein extracts from *ppi2* protoplasts transformed with *T7:Toc159GM* were included in the analysis. Consistent with the RT-PCR data, both Hsc70-4 and CHIP proteins were present at much higher levels in *ppi2* plants than in wild-type plants (Figure 2D). Furthermore, the levels of these two proteins were slightly lower after transformation of *T7:Toc159GM* into *ppi2* protoplasts (Figure 2C). However, the reduction in the protein level was much less than the reduction in the transcript level, possibly reflecting the difference in the stabilities of mRNA transcripts and proteins.

### High Levels of Chloroplast-Destined Precursor Proteins Induce Hsc70-4 and CHIP in Protoplasts

To further confirm that high levels of chloroplast precursors, but not abnormal chloroplast development due to defects in protein import, are responsible for Hsc70-4 induction in *ppi2* plants, we examined the effect of two green fluorescent protein (GFP) reporters, ribulose-1,5-bisphosphate carboxylase oxygenase small subunit-transit peptide (RbcS-tp):GFP and RbcS[T1A]:GFP, on Hsc70-4 induction in protoplasts from leaf tissues of wild-type plants. RbcS-tp:GFP that contains the RbcS transit peptide (TP) is efficiently imported into chloroplasts and produces almost no precursors (Lee et al., 2002). By contrast, RbcS[T1A]:GFP, which contained an RbcS-tp mutant that had Ala-substitutions of amino acids 2 to 11 (see Supplemental Figure 4 online), produced significant levels of precursor due to delayed chloroplastic import (Figure 3A, top panel) (Lee et al., 2006).

Protoplasts were transformed with *RbcS[T1A]:GFP* or *RbcS-tp:GFP*, and the total RNA from transformed protoplasts was used for RT-PCR analysis to determine the transcript levels of 13 Hsp70s. RbcS[T1A]:GFP induced significantly greater expression of all Hsc70 isoforms, except the most distantly related Hsc70-5, than RbcS-tp:GFP (Figure 3B). Induction was most prominent with Hsc70-4. However, *Hsp70-A*, *Hsp70-B*, *Hsp70-C*, *Bip-1*, two *mtHsp70s*, and two *cpHsp70s* were unaffected by RbcS[T1A]:GFP. These results suggest that high levels of chloroplast precursors induce the expression of Hsc70-4.

We examined the specificity of Hsc70-4 induction using two mitochondrial reporters, F1:GFP and F1m:GFP, which contain F1-ATPase- $\gamma$  presequence (F1) and an F1 mutant containing Ala substitutions of amino acids 46 to 50 and 56 to 60, respectively (see Supplemental Figure 4 online). F1:GFP primarily produced processed forms, with a small fraction of precursors. By contrast, F1m:GFP generated primarily precursors, with a minor fraction of the processed form (Figure 3A, top panel) (Jin et al., 2003). Neither F1m:GFP nor F1:GFP induced Hsc70s to levels higher than those induced by RbcS-tp:GFP (Figure 3B), indicating that the induction is specific to chloroplast precursors. The reporter genes were expressed to equal levels, as determined by RT-PCR (Figure 3A, bottom panel).

Next, we examined whether CHIP was induced by inefficiently imported RbcS[T1A]:GFP in protoplasts. Total RNA from transformed protoplasts was used for RT-PCR analysis using CHIP-

specific primers. As observed with Hsc70 isoforms, expression of CHIP was induced by RbcS[T1A]:GFP, but not RbcS-tp:GFP (Figure 3B). Interestingly, CHIP was also induced slightly by F1m:GFP, indicating that CHIP may play a role in other protein quality control responses (Shen et al., 2007a, 2007b).

To gain further insight into the induction of Hsc70-4 and CHIP by RbcS[T1A]:GFP, we followed the time course of their induction in protoplasts transformed with *RbcS[T1A]:GFP*. Total RNA from transformed protoplasts at various time points after transformation was subjected to RT-PCR using GFP-specific primers. In protoplasts transformed with *RbcS[T1A]*, both Hsc70-4 and CHIP transcript levels increased rapidly and reached a maximum level at 3 and 9 h after transformation, respectively. Hsc70-4 transcripts declined 3 h after transformation. By contrast, CHIP transcripts remained at the maximum level until 9 h after transformation before declining to lower levels (Figure 3C). As a control, we examined induction of Hsc70-4 and CHIP in protoplasts transformed with *RbcS-tp:GFP*. The transcript levels of Hsc70-4 and CHIP did not change significantly over the time course of the experiment. In addition, we confirmed that *RbcS[T1A]:GFP* and *RbcS-tp:GFP* displayed an identical expression pattern in protoplasts. These results again confirmed that RbcS[T1A]:GFP, but not RbcS-tp:GFP, induced the expression of Hsc70-4 and CHIP.

To gain insight into the spectrum of genes that are induced by unimported chloroplast precursors, we performed RT-PCR analysis using total RNA from *RbcS[T1A]:GFP*- and *RbcS-tp:GFP*-transformed protoplasts. We focused on the import receptor genes *Toc33*, *Toc34*, *Tic110*, *Toc75*, and *Toc159*, the proteasome subunit genes *RPN1*, *RPN5B*, and *RPN10*, and the heat shock transcription factor *HSF2A*. Among the genes we examined, *HSF2A*, *CHIP*, *RPN1*, *RPN5B*, and *RPN10* were induced to higher levels in *RbcS[T1A]:GFP*-transformed protoplasts compared with *RbcS-tp:GFP*-transformed protoplasts (see Supplemental Figure 5 online).

### Hsc70-4 Causes Degradation of Unimported Chloroplast-Targeted Reporter Proteins

The high levels of Hsc70-4 may play a role in either enhancing protein import into chloroplasts, as observed with spinach (*Spinacia oleracea*) chloroplast outer membrane-associated SCE70 (Com70) and Hsp70 in the guidance complex (Ko et al., 1992; Kourtz and Ko, 1997; Jarvis and Soll, 2002), or degradation of unimported precursors, as observed in protein quality control in animal and yeast cells (Figure 1; Esser et al., 2004). We examined the effect of high Hsc70-4 levels on protein import into chloroplasts using various chloroplast-targeted GFP proteins (RbcS-tp:GFP, Cab-tp:GFP [GFP fused to Cab TP], and RA-tp:GFP [GFP fused to ribulose-1,5-bisphosphate carboxylase/oxygenase activase TP]; see Supplemental Figure 4 online). In protoplasts, both RbcS-tp:GFP and Cab-tp:GFP were efficiently processed and imported into chloroplasts, whereas RA-tp:GFP yielded significant amounts of precursors in addition to the processed form (Figure 4A) (Lee et al., 2006, 2008). Protoplasts were transformed with the GFP reporter constructs together with *T7:Hsc70-4* or an empty expression vector *R6*. *T7:Hsc70-4* had no effect on the import of RbcS-tp:GFP and Cab-tp:GFP (Figure 4A). However, in

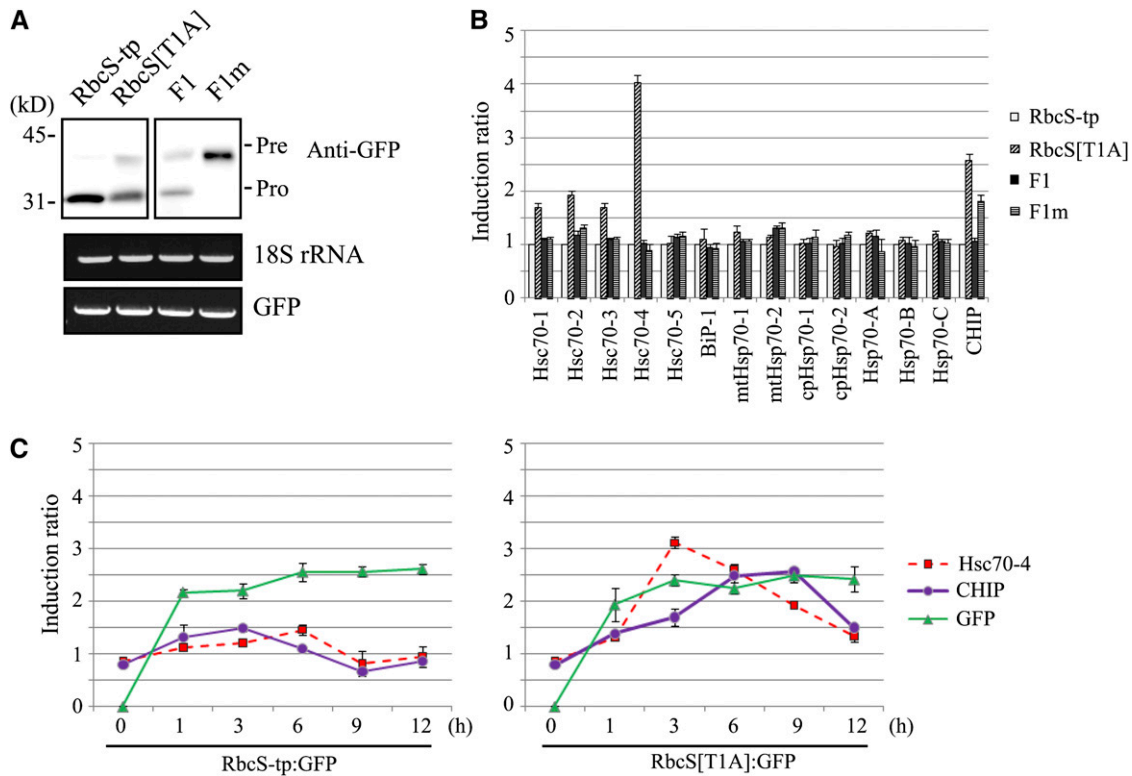


**Figure 3.** *Hsc70-4* and *CHIP* Were Induced by High Levels of Plastid Precursors.

(A) Protein gel blot and agarose gel analyses of reporters at protein and transcript levels in protoplasts. Protoplasts were transformed with the indicated constructs and reporter proteins were analyzed by protein gel blots using an anti-GFP antibody (top panel). Total RNA from protoplasts transformed with the indicated constructs was subjected to RT-PCR analysis using primers specific for *GFP* and *18S rRNA*. Amplified PCR fragments were analyzed by agarose gel electrophoresis (bottom panel). RbcS-tp, RbcS-tp:GFP; RbcS[T1A], RbcS[T1A]:GFP; F1, F1:GFP; F1m, F1m:GFP; Pre, precursor; Pro, processed forms. All TPs are fused to GFP.

(B) Protoplasts were transformed with the indicated constructs. Total RNA was prepared and subjected to RT-PCR analysis using gene-specific primers for 13 *Hsp70* homologs. The intensity of the amplified products after agarose gel electrophoresis was quantified and is presented relative to RbcS-tp:GFP. Three independent transformation experiments were performed. Error bar indicates SE ( $n = 3$ ). RbcS-tp, wild-type RbcS-tp; RbcS[T1A], RbcS-tp with Ala substitutions of the first 10-amino acid segment; F1 and F1m, presequence of mitochondrial F1-ATPase- $\gamma$  subunit and an Ala substitution mutant, respectively. All RbcS TPs and mitochondrial presequences were fused to GFP.

(C) Time course of *Hsc70-4* and *CHIP* induction in protoplasts. Protoplasts were transformed with *RbcS-tp:GFP* or *RbcS[T1A]:GFP*. Total RNA from the transformed protoplasts was prepared at the indicated time point after transformation and used for RT-PCR using specific primers for *GFP*, *Hsc70-4*, or *CHIP*. Three independent experiments were performed. Error bar indicates SE ( $n = 3$ ).

[See online article for color version of this figure.]

*T7:Hsc70-4*-transformed protoplasts, RA-tp:GFP yielded no precursors. Interestingly, the level of processed forms in *T7:Hsc70-4*-transformed protoplasts was nearly the same as that in the *R6*-transformed control, suggesting that *Hsc70-4* causes RA-tp:GFP precursor degradation. To further explore this possibility, we examined the effect of *Hsc70-4* on the import of RbcS-tp mutant constructs, RbcS[T1A]:GFP, RbcS[T1A]+1S:GFP, RbcS[T1A]+2S:GFP, and RbcS[T1A]+3S:GFP. The latter three mutants contain one, two, or three Ser residues, respectively, in the RbcS[T1A] background (see Supplemental Figure 4 online). All of these mutants produced significant amounts of precursors. However, they were slowly imported into chloroplasts (Figure 4B) (Lee et al., 2006). In *T7:Hsc70-4*-transformed protoplasts, the mutants produced almost undetectable precursor levels and almost no mature proteins (Figure 4B). The absence of mutant protein was not due to

transcriptional defects, since the *RbcS[T1A]:GFP* transcript levels were comparable to those of *RbcS-tp:GFP*, regardless of whether or not *T7:Hsc70-4* was expressed (see Supplemental Figure 6 online). One possible explanation for this is that the precursors of these slowly imported mutant reporter proteins were rapidly degraded in the cytosol.

We further examined the effect of *T7:Hsc70-4* on various Cab-tp mutant constructs. Cab[T3A]:GFP, Cab[T4A]:GFP, and Cab[T5A]:GFP contained Ala substitutions in the third, fourth, and fifth 10-amino acid segments, respectively, of Cab-tp and produced primarily precursors when transformed into protoplasts (Lee et al., 2008). In *T7:Hsc70-4*-transformed protoplasts, the precursors of these reporters were almost undetectable except for Cab[T4A]:GFP (Figure 4C). However, *Hsc70-4* had no effect on the levels of Cab[T2A]:GFP and Cab[T6A]:GFP, which

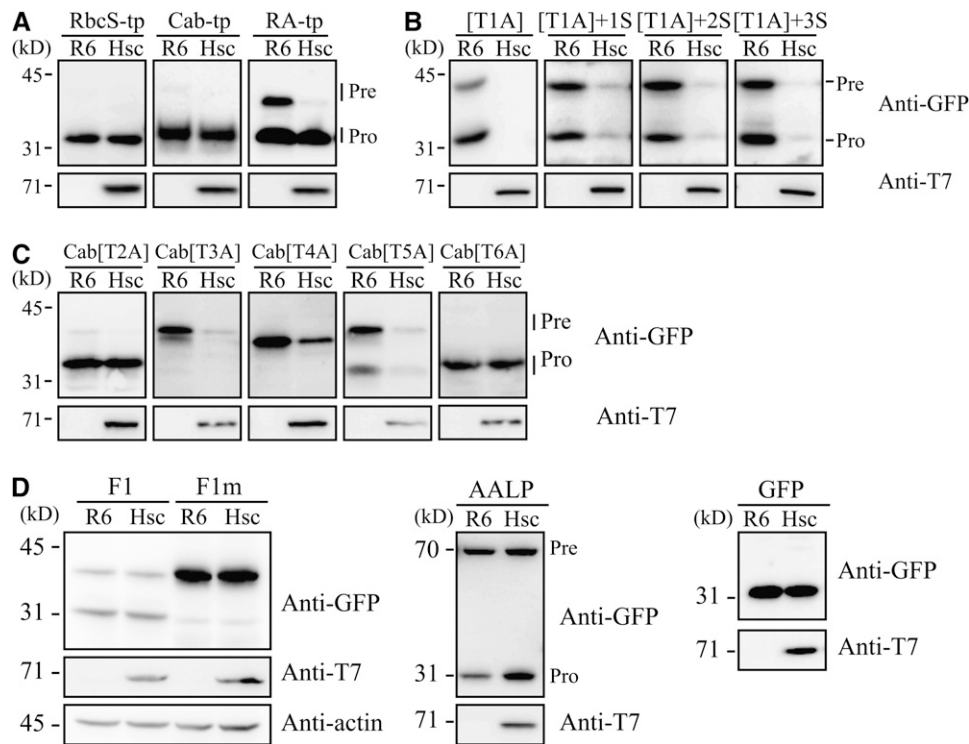


**Figure 4.** Hsc70-4 Causes Degradation of Unimported Plastid Precursors.

**(A) to (C)** Effect of Hsc70-4 on chloroplast-targeted GFP reporters. Wild-type TPs of RbcS, Cab, and RA **(A)**, mutant TPs of RbcS-tp **(B)**, and mutant TPs of Cab-tp **(C)** were used to deliver GFP into chloroplasts in protoplasts. The indicated reporter constructs were introduced into protoplasts together with *T7:Hsc70-4* (Hsc, 10  $\mu$ g) or *R6* (empty expression vector, 10  $\mu$ g), and protein levels were examined by protein gel blots using anti-GFP and anti-T7 antibodies. Pre, precursor; Pro, processed form. [T1A]+1S, [T1A]+2S and [T1A]+3S, one to three Ser residues in the RbcS[T1A] background; in Cab [T2A] to Cab[T6A], the second to sixth 10-amino acid segments were substituted with Ala residues (see Supplemental Figure 4 online). All TPs were fused to GFP.

**(D)** Specificity of Hsc70-4-mediated protein degradation. Protoplasts were transformed with the indicated constructs, and protein levels were determined by protein gel blots using anti-GFP, anti-T7, and anti-actin antibodies. Actin was assessed as a loading control. Hsc, *T7:Hsc70-4*; AALP, AALP:GFP.

contained Ala substitutions in the second and sixth 10-amino acid segments, respectively, and were efficiently imported into chloroplasts. These results indicate that Hsc70-4 causes the degradation of unimported or inefficiently imported precursors.

To test the specificity of Hsc70-4-mediated protein degradation, we examined whether Hsc70-4-mediated degradation was specific to chloroplast proteins. *Hsc70-4* was transformed into protoplasts together with mitochondrial, vacuolar, or cytosolic reporters. *T7:Hsc70-4* did not cause precursor degradation of the mitochondrial reporters F1:GFP or F1m:GFP, despite the high protoplasmic levels of mitochondrial reporter protein precursors, particularly F1m:GFP. Furthermore, *T7:Hsc70-4* did not induce degradation of the vacuolar protein AALP or of cytosolic GFP (Figure 4D). These results suggest that Hsc70-4 is chloroplast protein specific.

#### Sequence Motifs in T2 and T6 of RbcS-tp Are Involved in Both Hsc70-4-Mediated Precursor Degradation and Hsc70-4 Induction

To identify the sequence motif(s) that mediates *Hsc70-4* induction and precursor degradation, serial overlapping 20-

amino acid segments of RbcS-tp were fused to GFP (Figure 5A). Since these constructs contained only a fragment of RbcS-tp, they were not imported into chloroplasts but stayed in the cytosol as indicated by strong cytosolic GFP signals in protoplasts (see Supplemental Figure 7 online). Next, these constructs were introduced into protoplasts together with *T7:Hsc70-4* or *R6*. As a control, GFP alone was included. In *T7:Hsc70-4*-transformed protoplasts, RbcS[02]:GFP, RbcS [13]:GFP, RbcS[46]:GFP, and RbcS[57]:GFP levels were reduced to 25, 36, 38, and 56%, respectively, of the corresponding *R6* controls (Figures 5B and 5C). However, *T7:Hsc70-4* did not reduce the levels of RbcS[24]:GFP, RbcS [35]:GFP, or RbcS[68]:GFP. In addition, *T7:Hsc70-4* did not affect the level of GFP alone. These results suggest that T2 and T6 contain the sequence motif for Hsc70-4-mediated precursor degradation.

We generated additional GFP reporters using the N-terminal 15-amino acids of RbcS-tp (N15) or the N15 mutant derivatives N15-1A, N15-2A, and N15-3A, which had Ala substitutions in the first, second, and third 5-amino acid segments, respectively (Figure 5A). Again in protoplasts, these reporter proteins



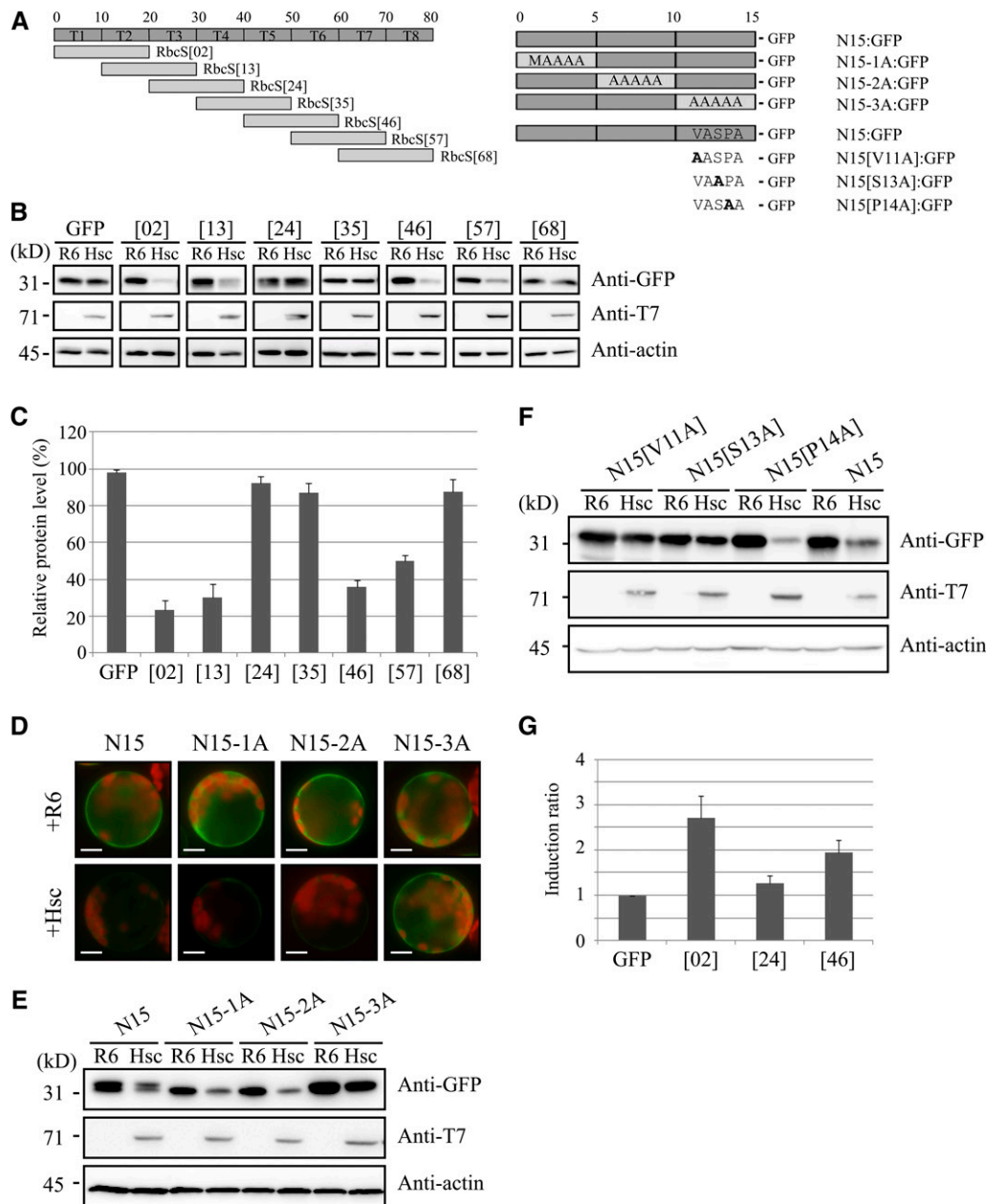


**Figure 5.** Specific Sequence Motifs of RbcS-tp Are Involved in Both Hsc70-4-Mediated Precursor Degradation and Hsc70-4 Induction.

**(A)** Schematic representation of GFP reporter constructs. A series of overlapping 20-amino acid segments (amino acid 1 to 20 [02], 11 to 30 [13], 21 to 40 [24], 31 to 50 [35], 41 to 60 [46], 51 to 70 [57], and 61 to 80 [68]) of RbcS-tp were fused to GFP at their N terminus. The N-terminal 15-amino acid segment of RbcS-tp was divided into three 5-amino acid blocks, and each block was substituted with Ala residues, with the exception of the initiating Met in the first 5-amino acid block. In the third 5-amino acid segment, V, S, and P at positions 11, 13, and 14 were replaced with Ala to generate N15 [V11A], N15[S13A], and N15[P14A], respectively.

**(B)** and **(C)** Identification of the RbcS-tp domain involved in Hsc70-4-mediated degradation. Protoplasts were transformed with the indicated constructs, and proteins were analyzed by protein gel blotting using anti-GFP, anti-T7, and anti-actin antibodies. Actin was analyzed as a loading control **(B)**. Band intensity was quantified using a software-equipped LAS3000 system (Fujifilm). The data show the percentage of intensity of T7:Hsc70-4 relative to R6. Error bar indicates SE ( $n = 3$ ) **(C)**.

**(D)** to **(F)** Fine mapping of the sequence motif involved in Hsc70-4-mediated protein degradation. The indicated constructs were introduced into protoplasts together with *T7:Hsc70-4* or *R6*, and protein levels were analyzed by monitoring the GFP signal intensity with a fluorescence microscope **(D)** or protein gel blotting using anti-GFP and anti-T7 antibodies **(E)** and **(F)**. Actin was analyzed as a loading control **(E)** and **(F)**. All TPs were fused to GFP. Red and green signals in **(D)**, autofluorescence of chlorophyll and GFP, respectively; R6, empty expression vector; Hsc, *T7:Hsc70-4*. Bars in **(D)** = 20  $\mu\text{m}$ .

**(G)** Identification of the sequence motif for induction of Hsc70-4. Total RNA from protoplasts that had been transformed with the indicated constructs was used for RT-PCR analysis. The intensity of bands was quantified. Error bar indicates SE ( $n = 3$ ). [02], RbcS[02]; [24], RbcS[24]; [46], RbcS[46]. All these transit peptides are fused to GFP. GFP, GFP alone.



produced strong GFP signals in the cytosol (Figure 5D), indicating that the 15–amino acid fragment of RbcS-tp at the N terminus of GFP did not affect the folding of the GFP domain. To further narrow down which sequence motif is involved in Hsc70-4–mediated protein degradation, we examined the effect of Hsc70-4 on these reporters. These constructs were introduced into protoplasts together with *T7:Hsc70-4* or *R6*, and the intensity of GFP signals was examined using a fluorescence microscope. In the presence of *T7:Hsc70-4*, the GFP signals of N15:GFP, N15-1A:GFP, and N15-2A:GFP were greatly reduced compared with the corresponding *R6* control samples (Figure 5D). However, *T7:Hsc70-4* did not affect the GFP signal intensity of N15-3A:GFP, indicating that the third 5–amino acid segment contains the sequence motif for Hsc70-4–mediated protein degradation. To further confirm this, protein extracts from the transformed protoplasts were subjected to protein gel blot analysis using the anti-GFP antibody. Consistent with the results obtained from the image analysis, *T7:Hsc70-4* reduced the levels of N15:GFP, N15-1A:GFP, and N15-2A:GFP, but not of N15-3A:GFP, confirming that the Hsc70-4–specific sequence motif is located between amino acids 11 and 15 of N15 (Figure 5E). To identify the individual amino acids involved in Hsc70-4–mediated degradation, we generated N15[V11A]:GFP, N15[S13A]:GFP, and N15[P14A]:GFP, which had Alasubstitutions of 11V, 13S, and 14P, respectively, in N15 (Figure 5A). Of these mutants, only N15[P14A]:GFP was susceptible to Hsc70-4–mediated degradation (Figure 5F), indicating that 11V and 13S of RbcS-tp are essential for Hsc70-4–mediated degradation.

Next, we identified the sequence motif involved in *Hsc70-4* induction. We hypothesized that the sequence motif involved in precursor degradation also plays a role in *Hsc70-4* induction. To test this hypothesis, protoplasts were transformed with *RbcS[02]:GFP*, *RbcS[24]:GFP*, *RbcS[46]:GFP*, or *GFP* alone, and the *Hsc70-4* induction was examined by RT-PCR using the total RNA from protoplasts. *RbcS[02]:GFP* and *RbcS[46]:GFP* increased significantly *Hsc70-4* transcript levels compared with that of *GFP* alone (Figure 5G). However, *RbcS[24]:GFP* failed to induce *Hsc70-4*, indicating that T2 and T6 contain the sequence motif for *Hsc70-4* induction, as observed with Hsc70-4–mediated proteolysis.

In a previous study, Hsp70 binds to the transit peptides of plastid proteins (Ivey and Bruce, 2000). Indeed, it has been shown that pea (*Pisum sativum*) Hsp70 homolog chloroplast stress seventy (CSS1) has a strong binding site with 24–amino acid residues of pea RbcS-tp (Ivey et al., 2000). Thus, one possibility is that Hsc70-4 may bind directly to the specific sequence motif to mediate precursor degradation. To examine whether Hsc70-4 interacts directly with the Hsc70-4–responsive sequence motif of RbcS-tp, *T7:Hsc70-4* was transformed into protoplasts together with *RbcS[02]:GFP* or *GFP* alone, and protein extracts from transformed protoplasts were subjected to immunoprecipitation with an anti-GFP antibody. The immunoprecipitates were analyzed by protein gel blotting using anti-GFP and anti-T7 antibodies. *T7:Hsc70-4* coimmunoprecipitated with *RbcS[02]:GFP*, but not *GFP* (Figure 6A), indicating that Hsc70-4 interacts with T2 of RbcS-tp.

We also performed protein pull-down experiments using MBP:Hsc70-4 (Hsc70-4 fused to maltose binding protein) and four

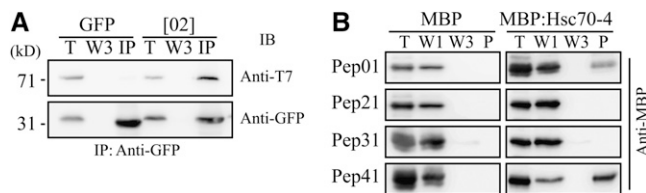


**Figure 6.** *T7:Hsc70-4* Directly Interacts with the Sequence Motif Involved in Hsc70-4–Mediated Protein Degradation.

Interaction between RbcS-tp and Hsc70-4. *T7:Hsc70-4* was transformed into protoplasts together with *GFP* or *RbcS[02]:GFP* ([02]), and protein extracts were subjected to immunoprecipitation using an anti-GFP antibody. Immunoprecipitates were analyzed by protein gel blots using anti-T7 and anti-GFP antibodies (**A**). For protein pull-down experiments, oligopeptides representing regions of RbcS-tp were cross-linked to an affi-gel and then incubated with recombinant purified MBP:Hsc70-4 or MBP alone. Proteins were precipitated and analyzed by protein gel blots using an anti-MBP antibody (**B**). T, 10% of total extract or recombinant protein; IB, immunoblot; IP, immunoprecipitation; P, precipitate; W1 and W3, first and third washing fractions, respectively.

synthetic oligopeptides (Pep01, Pep21, Pep31, and Pep41) corresponding to amino acids 1 to 20, 21 to 40, 31 to 50, and 41 to 60, respectively, of RbcS-tp (see Supplemental Figure 8A online). MBP:Hsc70-4 or MBP alone (see Supplemental Figure 8B online) was incubated with oligopeptides cross-linked to an Affi-gel. Bound proteins were precipitated and analyzed by protein gel blotting using an anti-MBP antibody. MBP:Hsc70-4 was detected in the precipitates of Pep01 and Pep41, but not of Pep21 or Pep31 (Figure 6B), indicating that Hsc70-4 binds directly to T2 and T6.

### Hsc70-4 Engages the UPS for Chloroplast-Destined Precursor Degradation

We examined whether the UPS is involved in the Hsc70-4–mediated degradation of chloroplast-targeted precursors in protoplasts (Hershko et al., 2000; Smalle and Vierstra, 2004). Since the first 20–amino acid segment of RbcS-tp contained the Hsc70-4 binding site and was sufficient for Hsc70-4–mediated protein degradation, we used *RbcS[02]:GFP* as a reporter protein. Protoplasts transformed with *T7:Hsc70-4* and *RbcS[02]:GFP* were treated with MG132 or UCH-L3, which are inhibitors of the 26S proteasome and deubiquitination, respectively (Lee and Goldberg, 1998; Liu et al., 2003). Protein levels were examined by protein gel blotting. Both MG132 and UCH-L3 almost completely suppressed the Hsc70-4–mediated proteolysis of *RbcS[02]:GFP* (Figures 7A to 7C), strongly suggesting that ubiquitin and the 26S proteasome are involved in the degradation process.

We also examined the ubiquitination of *RbcS[02]:GFP*. Protoplasts transformed with *RbcS[02]:GFP* or *GFP* were incubated with MG132 or DMSO as a control. Protoplast extracts were subjected to immunoprecipitation using an anti-GFP antibody, followed by protein gel blot analysis of immunoprecipitates using an anti-ubiquitin antibody. The expression of *RbcS[02]:GFP*, but not *GFP* alone, resulted in the appearance of ubiquitin-positive

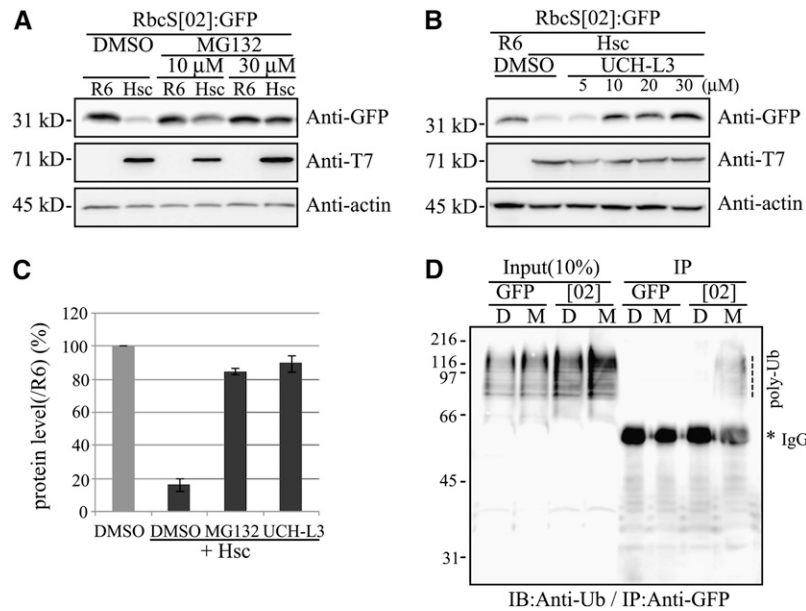


**Figure 7.** Hsc70-4 Engages the Ubiquitin/26S Proteasome Pathway for Protein Degradation.

(A) to (C) Inhibition of reporter protein degradation. The indicated constructs were transformed into protoplasts, which were then treated with MG132 (A) or UCH-L3 (B). DMSO was included as a vehicle control. Protein levels were determined by protein gel blot analysis using the indicated antibodies. Actin was analyzed as a loading control. The intensity of the protein bands was quantified, and data are percentage of intensity relative to R6 + DMSO. D, DMSO; M30, MG132 (30 μM); U30, UCH-L3 (30 μM); Hsc, T7:Hsc70-4. Error bar indicates SE ( $n = 3$ ) (C).

(D) Ubiquitination of RbcS[02]:GFP. Protein extracts from protoplasts transformed with the indicated constructs were subjected to immunoprecipitation using an anti-GFP antibody. Immunoprecipitates and total extract (10%) were analyzed by protein gel blots using an anti-ubiquitin antibody. [02], RbcS [02]:GFP; D, DMSO; M, MG132; IB, immunoblotting; IP, immunoprecipitates; Anti-Ub, anti-ubiquitin antibody; dashed line, polyubiquitinated RbcS[02]:GFP; asterisk, IgG heavy chain.

high molecular weight complexes, which is a typical pattern for polyubiquitinated proteins (Figure 7D). These results confirm that RbcS[02]:GFP is ubiquitinated.

### CHIP Interacts with Hsc70-4 and Is Involved in Hsc70-4-Mediated Protein Degradation

In animal cells, the E3 ligase CHIP is involved in Hsc70-mediated protein degradation (Ballinger et al., 1999; Connell et al., 2001). In plant cells, CHIP interacts with RbcS and Cab and ubiquitinates the chloroplast-targeted proteins FtsH1 and ClpP4 (Luo et al., 2006; Shen et al., 2007a, 2007b). Hsc70-4 also contains a conserved C-terminal CHIP-interacting motif. In addition, CHIP was highly induced in *ppi2* plants and in protoplasts expressing inefficiently imported chloroplast-destined reporter proteins (Figures 2C and 2D). Furthermore, Lhcb4 was ubiquitinated in *ppi2* plants (Figure 1B). Together, these observations suggest that CHIP may ubiquitinate chloroplast-destined precursors for degradation when these precursors are not efficiently imported into chloroplasts.

To test whether CHIP is involved in Hsc70-4-induced protein degradation, we examined the interaction between CHIP and Hsc70-4 by coimmunoprecipitation. CHIP coimmunoprecipitates with cytosolic Hsp70 (Shen et al., 2007a). Protein extracts from protoplasts cotransformed with *CHIP:HA* and *T7:Hsc70-4* were used for immunoprecipitation with an anti-HA antibody. An

unrelated small GTP binding protein Arf1:HA was used as a negative control. The immunoprecipitates were analyzed by protein gel blotting using an anti-T7 antibody. T7:Hsc70-4 was detected in the precipitates of CHIP:HA, but not of Arf1:HA (Figure 8A), indicating that CHIP interacts with Hsc70-4. To further examine this interaction, purified MBP:Hsc70-4, MBP:Hsc70-4N, or MBP:Hsc70-4C was incubated with purified His:CHIP. MBP:Hsc70-4N and MBP:Hsc70-4C contain the N- and C-terminal half of Hsc70-4, respectively. Proteins were precipitated with Ni<sup>+</sup>-NTA agarose, and the precipitates were analyzed by protein gel blotting using anti-MBP. The full-length and C-terminal constructs of Hsc70-4 were detected in the precipitates, indicating that CHIP directly interacts with the C-terminal region of Hsc70-4 (Figure 8B).

We next examined the effect of CHIP on RbcS[02]:GFP degradation. *RbcS[02]:GFP* and *T7:Hsc70-4* were transformed into protoplasts together with *T7:CHIP* or *T7:TPR*, and Hsc70-4-mediated protein degradation was examined in the protoplasts. TPR, a deletion mutant that contains only the N-terminal TPR domain of CHIP (which interacts with Hsp70; Nelson et al., 2006), was included as a dominant-negative mutant (Jiang et al., 2001). Coexpression of both T7:CHIP and T7:Hsc70-4 slightly further increased the extent of Hsc70-4-induced reporter protein degradation compared with the expression of T7:Hsc70-4 alone (Figure 8C, compare lane 5

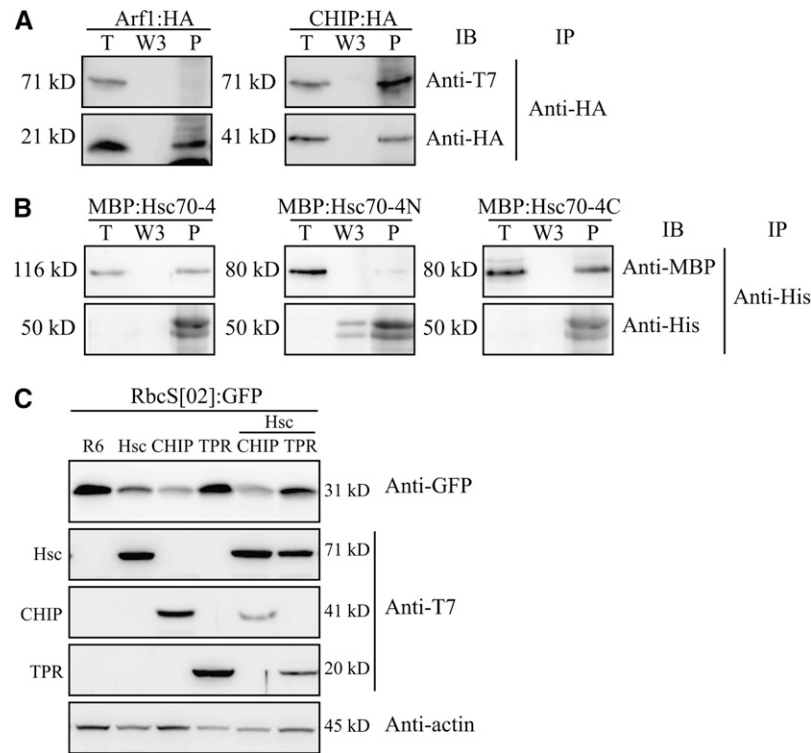


**Figure 8.** CHIP Interacts with Hsc70-4 and Plays a Critical Role in Hsc70-4-Induced Protein Degradation.

**(A)** Interaction between Hsc70-4 and CHIP. Protoplasts were transformed with the indicated constructs and protein extracts were used for immunoprecipitation using an anti-HA antibody. Precipitates were analyzed by immunoblotting using anti-HA and anti-T7. Arf1:HA was used as a negative control. T, 10% of total protein extracts; W3, third wash supernatant; P, precipitates; IP, immunoprecipitation; IB, immunoblotting.

**(B)** Protein pull-down experiment. Purified recombinant MBP:Hsc70-4, MBP:Hsc70-4N, or MBP:Hsc70-4C were incubated with His:CHIP bound to Ni<sup>2+</sup>-NTA agarose. Precipitates were analyzed by protein gel blotting using anti-MBP and anti-His antibodies. T, 10% of total protein extracts; W3, the third wash supernatant; P, precipitates.

**(C)** Inhibition of Hsc70-4-mediated degradation by the TPR domain. Protein extracts from protoplasts transformed with the indicated constructs were analyzed by protein gel blotting using anti-GFP and anti-T7. R6, empty vector; CHIP, T7:CHIP; TPR, T7:TPR domain construct.

with lane 2). By contrast, coexpressed T7:TPR suppressed Hsc70-4-mediated RbcS[02]:GFP degradation (Figure 8C, lane 6), indicating that CHIP plays a critical role in Hsc70-4-mediated degradation.

### Hsc70s Are Essential for Normal Plant Development

We also examined the physiological role of Hsc70-4 in plants. Since an *Hsc70-4* mutant was not available, we generated transgenic plants harboring an *Hsc70-4* RNA interference (RNAi) construct in the wild-type plant background; however, these plants did not produce any noticeable phenotype, likely due to the functional redundancy of Hsc70 isoforms (Noël et al., 2007). This possibility is supported by the evidence that other Hsc70 isoforms are also induced in *ppi2* plants and by the inefficient import of chloroplast-destined reporter proteins into protoplasts (Figures 2B and 2D). Accordingly, we isolated the T-DNA insertion mutants *hsc70-1* and *hsc70-2* (see Supplemental Figures 9A and 9B online), which also did not display any visible phenotype (see Supplemental Figure 9C online) (Noël et al., 2007).

We next generated transgenic plants harboring an *Hsc70-4* RNAi construct in the *hsp70-1* background. The RNAi construct contained a DNA fragment encoding the Hsc70-4 C-terminal region (see Supplemental Figure 9D online). *Hsp70-1* mutant plants were generated by T-DNA insertion and thus contained the kanamycin resistance gene as a selection marker. We used the pART vector, which also contains the kanamycin resistance gene (Wesley et al., 2001), and empirically determined the kanamycin concentration to which *hsp70-1* plants were sensitive (50 mg/L kanamycin). This concentration was used to select multiple independent transgenic lines (RNAi plants), which contained developmentally defective seedlings in their T1 population. The Hsc70 levels in these RNAi lines were examined by protein gel blotting using an anti-Hsc70-4 antibody (Figure 9A). Hsc70-4 levels were greatly reduced in RNAi plants. To further confirm the low levels of Hsc70-4, we examined transcript levels of Hsc70-4 and other Hsp70 isoforms in RNAi plants (line number 56). The *Hsc70-4* and *Hsc70-1* transcripts were undetectable, and *Hsc70-2* transcripts were reduced to lower levels than those found in *hsc70-1* mutants (see Supplemental Figure 10 online). However, the transcript levels of the other Hsp70 homologs were unaffected in RNAi plants,

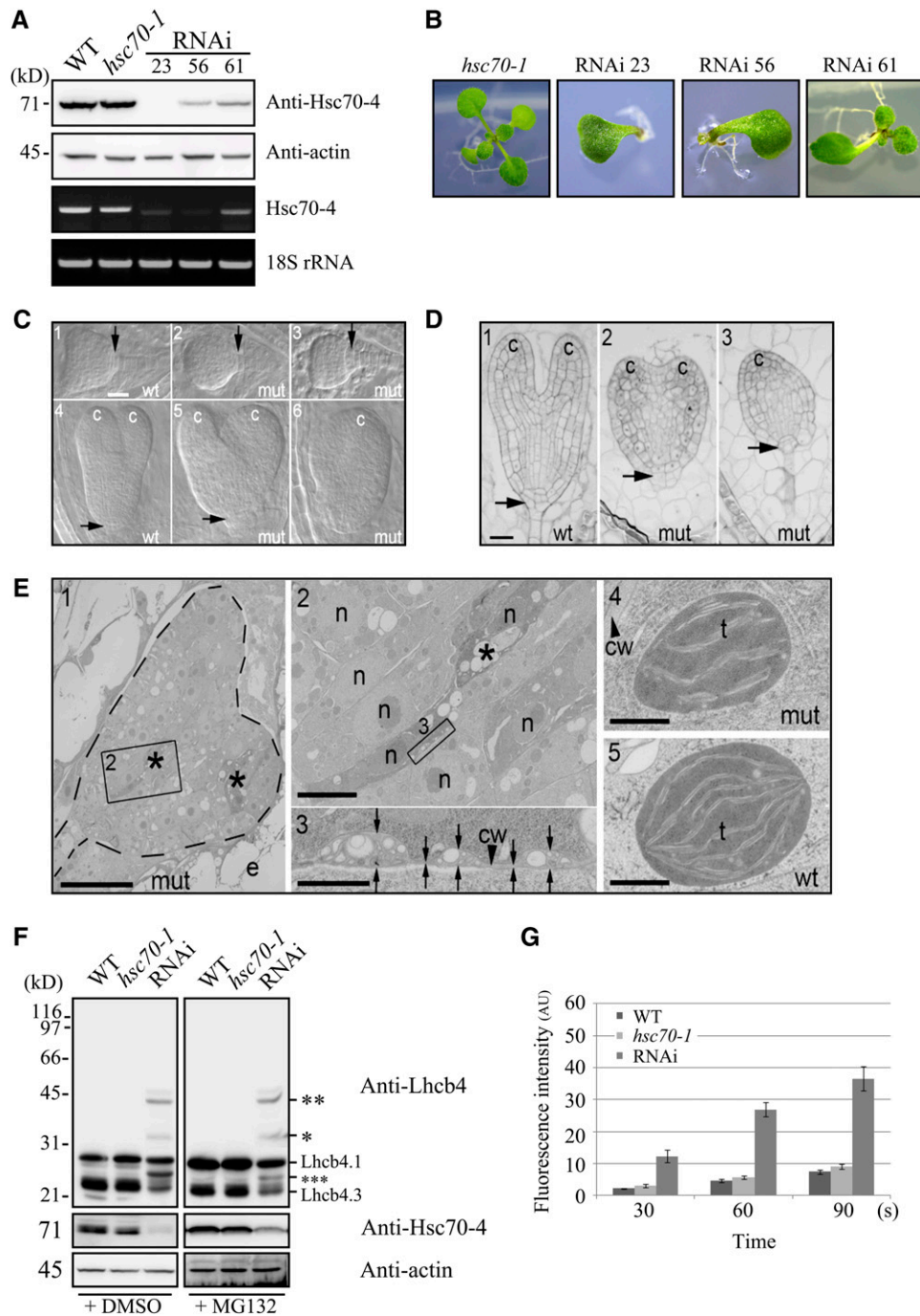


**Figure 9.** RNAi(Hsc70-4)*hsc70-1* Transgenic Plants Display Developmental Defects and High Levels of ROS.

**(A)** Protein gel blot and RT-PCR analyses of RNAi plants. Protein extracts from cotyledons of *hsc70-1* and RNAi plants (1 week old) were analyzed by protein gel blots using anti-Hsc70-4 and anti-actin antibodies (top two panels). In addition, total RNA from RNAi, wild-type, and *hsc70-1* plants was used for RT-PCR analysis using *Hsc70-4* and *18S rRNA*-specific primers (bottom two panels). The images of PCR products are representative of three independent experiments. Numbers indicate independent transgenic lines. RNAi, RNAi plants.

**(B)** Phenotype of RNAi plants. Plants were grown on MS plates for 3 weeks.

**(C) to (E)** Light and electron microscopy analysis of RNAi embryos. **(C1) to (C6)** Whole-mount preparations after clearing (embryo stages: 1 to 3, late-globular/heart; 4 to 6, torpedo). Differential interference contrast optics. mut, RNAi plant (line 56); c, cotyledon; arrow, root pole. **(D1) to (D3)** show semithin and **(E1) to (E5)** ultrathin resin sections of heart-stage embryos observed by light microscopy **(D)** or transmission electron microscopy **(E)**. Note single cotyledon (c) in D3. **(E1)** Overview of embryo (outlined); **(E2)** and **(E3)** higher magnifications of boxed areas in **(E1)** and **(E2)**, respectively; **(E4)**

suggesting that the developmental defects in RNAi plants were due to low levels of multiple Hsc70 isoforms.

Morphologically, RNAi seedlings displayed varying degrees of developmental defects, having only one cotyledon with or without a shoot meristem (Figure 9B). The severity of developmental defects correlated with the Hsc70 level detected by an anti-Hsc70-4 antibody (Figures 9A and 9B). We examined whether these observed developmental defects were inherited by subsequent generations. RNAi plants with a normal morphology were screened from the T1 generation of RNAi lines on Murashige and Skoog (MS) agar plates containing 50 mg/L kanamycin, and the T2 generation of these lines was planted on MS plates or soil. Approximately 24% of the T2 plants displayed developmental defects (see Supplemental Figure 11 online), raising the possibility that homozygotes, but not hemizygotes, of RNAi plants display developmental defects. This is consistent with the observation that the developmental defects were correlated with Hsc70 levels.

To examine the morphological defects in detail, RNAi embryos from two lines (#56 and #61) that exhibited a strong seedling phenotype were examined by light and electron microscopy. Although there was some phenotypic variability, we consistently observed strong deviations from wild-type embryo development. Cell division was irregular, resulting in abnormalities such as single cotyledons, unequal or fused cotyledons, and abnormal root poles (Figures 9C and 9D). These irregular cell divisions were indicative of cell death at specific positions in the embryo. Indeed, electron microscopy revealed evidence of degenerating cells and membrane vesicles between cells, possibly the debris of dead cells (Figure 9E). These results strongly suggest that the removal of unimported precursors by Hsc70s is essential for normal cell viability and organized cell division, particularly during embryogenesis. Indeed, Hsc70-4 was highly expressed during embryogenesis when examined by  $\beta$ -glucuronidase (*GUS*) expression under the control of the *Hsc70-4* promoter in transgenic plants (see Supplemental Figure 12 online), consistent with public microarray data (<http://www.genevestigator.com>). However, despite the dramatic effect on embryogenesis, the chloroplast morphology in RNAi plants was not significantly altered. The density of thylakoid membranes in RNAi plants appeared to be slightly lower than that in the wild type. Together, these results suggest that Hsc70-4 may not play a direct role in chloroplast development (Figure 9E4 and 9E5). However, we cannot rule out the possibility that Hsc70-4 plays a direct or indirect role in the efficiency of chloroplastic protein import.

To gain insight into the underlying mechanisms of the RNAi plant phenotype, protein extracts from the cotyledons of wild-type, *hsc70-1*, and RNAi (56) plants that had been treated with DMSO or MG132 were analyzed by protein gel blotting using the anti-Lhcb4 antibody. The DMSO- and MG132-treated samples displayed identical protein gel blot patterns (Figure 9F). In RNAi plants, Lhcb4.1 and Lhcb4.3 proteins at 29 and 23 kD, respectively, were reduced to lower levels than those in *hsc70-1* and wild-type plants. Instead, additional bands were detected in RNAi plants. Among them, the 34- and 42-kD bands (indicated by \* and \*\* in Figure 9F) appeared to be identical to those observed in *ppi2* plants and may thus correspond to the precursor and monoubiquitinated precursor of Lhcb4.1. In addition, the new 26-kD band may correspond to the precursor of Lhcb4.3 (indicated by \*\*\* in Figure 9F). However, RNAi plants did not contain the high molecular weight polyubiquitinated Lhcb4 forms observed in MG132-treated *ppi2* plants, indicating that the low Hsc70-4 levels in RNAi plants was not sufficient to polyubiquitinate the excess Lhcb4 proteins. In the UPS pathway, only polyubiquitinated forms are degraded by 26S proteasomes (Esser et al., 2004). Thus, accumulation of the precursors and monoubiquitinated forms of Lhcb4 proteins in RNAi plants was consistent with the absence of polyubiquitinated Lhcb4 proteins. As a control, we determined actin levels using an anti-actin antibody. Our results suggest that Hsc70-4 is critical for the removal of excess precursors from the cytosol through polyubiquitination.

Finally, we examined the reactive oxygen species (ROS) levels in RNAi plants as indirect evidence for the cytotoxic effect exerted by high levels of unfolded precursors. ROS levels increase in response to stress (Apel and Hirt, 2004). Cotyledons were stained with 2',7'-dichlorofluorescein (DCF), and the intensity of green fluorescence was measured in situ. Fluorescent DCF signals were slightly increased in *hsc70-1* mutants compared with wild-type plants. RNAi plants contained eightfold higher fluorescence levels than wild-type plants (Figure 9G; see Supplemental Figure 13 online), indicating that RNAi plant cells have a high toxic burden due to reduced Hsc70s activity. These results suggest that high cytosolic levels of unfolded chloroplast precursors are cytotoxic and can cause cell death during embryogenesis, resulting in irregular cell division, single cotyledon formation, and failure to establish a shoot meristem. However, it is possible that Hsc70-4 may also play a role in enhancing the protein import efficiency of plastid proteins into chloroplasts when an excess amount of plastid-destined precursors exists in the cytosol.

#### Figure 9. (continued).

and (E5) proplastids. Asterisks in (E1) and (E2), degenerating cells. Note extracellular membrane vesicles between neighboring plasma membranes ((E3); arrows). CW (arrowhead in (E3)), cell wall; c, cotyledon; e, endosperm; n, nucleus; t, thylakoid. Bars = 20  $\mu$ m in (C1) and (D), 25  $\mu$ m in (E1), 5  $\mu$ m in (E2), 1  $\mu$ m in (E3), and 0.5  $\mu$ m in (E4) and (E5). Bar in (C1) also applies to (C2) to (C6).

(F) Lhcb4 levels. Protein extracts from cotyledons (1 week old) of *hsc70-1*, RNAi, and wild-type plants were analyzed by protein gel blots using the indicated antibodies. Actin was analyzed as a loading control. \* and \*\*, expected sizes of precursors and monoubiquitinated Lhcb4.1; \*\*\*, expected size of the Lhcb4.3 precursor.

(G) Levels of ROS. Cotyledons (1 week old) were stained with DCF for the indicated periods of time, and fluorescence intensity was measured by confocal laser scanning fluorescence microscopy (see Supplemental Figure 13 online). Fluorescence intensity was quantified. AU, arbitrary unit; error bars indicate SE ( $n = 3$ ).

## DISCUSSION

In this study, we demonstrated that plant cells prevent cytosolic accumulation of unfolded plastid-destined precursors through UPS-mediated precursor degradation. Both Hsc70-4, a cytosolic/nuclear Hsp70 subfamily isoform that is induced by heat shock and pathogens (Sung et al., 2001; Noël et al., 2007), and CHIP, an E3 ligase involved in regulating chloroplast protein levels under conditions of high light stress (Shen et al., 2007a, 2007b), play critical roles in this process. We name this novel mechanism the plastid precursor response (PPR). However, we cannot exclude the possibility that Hsc70-4 may also play a role in enhancing the protein import efficiency into chloroplasts when plant cells contain an excess amount of plastid-destined precursors in the cytosol. In this study, we focused on the role of Hsc70-4 in plastid precursor degradation when there was an excess amount of precursor protein in the cytosol.

The PPR displays many similarities and some differences to the unfolded protein response (UPR) in the endoplasmic reticulum (Hampton, 2000; Ma and Hendershot, 2001). In the UPR, unfolded or misfolded protein-mediated signaling pathway activation induces genes involved in the removal of unfolded or misfolded proteins. Unfolded proteins are then removed either by the action of chaperones assisting in their correct folding or by degradation through the UPS (Esser et al., 2004; Bukau et al., 2006). Similarly, high plastid precursor levels activate a signaling pathway that leads to the induction of genes such as *Hsc70-4*, *CHIP*, and the 26S proteasome subunits *RPN1*, *RPN5B*, and *RPN10*. Another process in the PPR is the proteolytic removal of unimported or inefficiently imported precursors. However, unlike the UPR, the PPR may not include a mechanism for assisting in the correct folding of precursors in the cytosol. Hsc70-4 and CHIP play critical roles in the PPR, as observed with Hsc70 in PQC in animal cells (Murata et al., 2001; McDonough and Patterson, 2003; Esser et al., 2004).

The *Arabidopsis* genome encodes 14 Hsp70 homologs that can be classified into multiple subfamilies according to their subcellular localizations (Lin et al., 2001; Sung et al., 2001). Hsc70-1 is a cytosolic-/nuclear-localized isoform that is highly induced by heat shock and is involved in various abiotic stress responses, immune responses, and plant development (Noël et al., 2007; Cazalé et al., 2009). The physiological roles of specific Hsc70 isoforms have not been easy to determine because these isoforms show significant functional redundancy. Furthermore, the elimination of multiple isoforms leads to lethality in *Arabidopsis* (Noël et al., 2007). Among the five Hsp70 isoforms, *Hsc70-4* was the most strongly induced in *ppi2* plants and also by import-defective plastid-destined reporter proteins in protoplasts. Currently, it is not fully understood whether the differential expression of individual Hsc70 isoforms at different conditions reflects any difference in their activity or mechanisms. Based on the expression pattern of *Hsc70-4*, we favor the idea that Hsc70-4 is primarily responsible for the removal of plastid-destined precursors. Hsc70-4 is likely also involved in other physiological processes.

Both Hsc70-4 and CHIP mediated plastid-destined precursor degradation in the cytosol. One possible scenario is that Hsc70-4 recognizes the target proteins for degradation, and CHIP sub-

sequently ubiquitinates Hsc70-4-bound proteins for degradation by the 26S proteasomes. Transit peptides do not fold into a specific structure in aqueous solution (Bruce, 2001). Despite the unstructured nature of the transit peptides, interestingly, Hsc70-4 recognized a specific sequence motif in the RbcS-tp. A previous study showed that pea Hsp70 homolog CSS1 has a strong binding site within the first 24 residues of pea RbcS-tp (Ivey et al., 2000). Similarly, Hsc70-4 has a specific binding site within the first 20 amino acid residues of *Arabidopsis* RbcS-tp. In fact, the sequence motif located between amino acids 11 and 15 in RbcS-tp functions as a signal for Hsc70-4-mediated degradation of GFP. These results strongly suggest that Hsc70-4 recognizes a specific sequence motif, but not the protein folding status, for the protein degradation. In the absence of cotransformed T7:Hsc70-4, N15:GFP and its three mutant derivatives (N15-1A:GFP, N15-2A:GFP, and N15-3A:GFP) produced strong GFP signals in the cytosol, confirming that the GFP domain folded correctly in these reporter proteins. Furthermore, consistent with this hypothesis, high levels of mitochondria-destined precursors neither induced Hsc70-4 expression nor were subjected to Hsc70-4-mediated degradation, even although mitochondrial precursors also navigate through the cytosol as unfolded proteins. This proposed mechanism represents an important distinction from PQC, in which chaperones recognize the unfolded protein, such as heat-denatured proteins (Esser et al., 2004). The folding-independent, sequence-specific recognition of plastid-destined precursor transit peptides by Hsc70-4 may reflect the fact that plastid precursors navigate through the cytosol as unfolded proteins and not as substrates for correct folding (Hampton, 2000).

The suggestion that Hsc70-4 recognizes a specific sequence motif in the TP raises the intriguing question of what determines whether a precursor is destined for degradation or for import into plastids. One very plausible scenario is that Hsc70-4 causes degradation of import-incompetent, but not import-competent, precursors. Precursors that are assembled into a guidance complex with 14-3-3 and Hsp70 are more efficiently imported into plastids (May and Soll, 2000). The Hsp70 isoform that was found to bind to transit peptide in a previous study (May and Soll, 2000) may be an ortholog of Hsc70-4 of *Arabidopsis*. Hsc70-4 may help assess whether the precursors are incorporated into guidance complexes, as a mechanism of determining import competence. It is possible that Hsc70-4 can interact with both the guidance factor and CHIP. Thus, one possible scenario is that when Hsc70-4 binds to the transit peptide together with the guidance factor, Hsc70-4 may facilitate the protein import into chloroplasts. By contrast, in the absence of the guidance factor binding to the transit peptide, Hsc70-4 may alternatively interact with CHIP, which in turn leads to the degradation of precursors. Consistent with this hypothesis, RbcS[T1A]:GFP and its mutant derivatives that are slowly imported into chloroplasts in protoplasts (Lee et al., 2006) were highly susceptible to Hsc70-4-mediated degradation.

Unfolded proteins in an aqueous environment tend to form highly cytotoxic nonspecific aggregates if they accumulate to high levels (Wickner et al., 1999; Hartl and Hayer-Hartl, 2002; Hatakeyama and Nakayama, 2003; Esser et al., 2004). Therefore, the amount of unfolded plastid precursors must be precisely

maintained below a threshold at which nonspecific protein aggregates can form. Retrograde signals from the plastid to the nucleus may help regulate the amount of precursors at the transcriptional level (Fernández and Strand, 2008). Alternatively, if the cellular plastid precursor level exceeds the protein import capacity of plastids, the excess precursors may be actively removed by protein degradation. The latter hypothesis is supported by several lines of evidence, including the strong induction of *Hsc70-4* and *CHIP* by high levels of plastid precursors, UPS-mediated plastid protein degradation in *ppi2* plants and wild-type protoplasts, and monoubiquitinated Lhcb4 precursor accumulation in RNAi plants.

We have demonstrated that Hsc70-4-mediated precursor degradation maintains low cytosolic precursor levels and is essential for proper plant development. The development of Hsc70-4 RNAi embryos was highly abnormal, potentially due to abnormal cell death during embryogenesis. In animal cells, when unfolded protein levels exceed a threshold, damaged cells are committed to a cell death mediated by ATF4 and ATF6 and by activation of the JNK/AP-1/Gadd153 signaling pathway (Kim et al., 2006). In plant cells, ROS levels are increased under biotic and abiotic stresses (Overmyer et al., 2003; Apel and Hirt, 2004; Cho et al., 2009). In particular, high ROS can induce programmed cell death upon pathogen infection (Overmyer et al., 2003; Apel and Hirt, 2004). In Hsc70-4 RNAi plants, we observed highly elevated levels of ROS. Similarly, high ROS levels produced by nonspecific cytotoxic plastid precursor aggregates may cause cell death during embryogenesis. The expression pattern of *Hsc70-4* and the phenotypes of Hsc70-4 RNAi plants indicate that Hsc70-4 plays a critical role during embryogenesis. This may be because cell death in embryogenesis has profound effects on plant development, as observed in Hsc70-4 RNAi plants.

## METHODS

### Microarray Analysis

Wild-type *Arabidopsis thaliana* (Columbia-0) and *ppi2* mutants were grown in MS media for 3 weeks in a culture room with 16-h/8-h light/dark cycles at 20°C with 70% relative humidity and transferred to liquid nitrogen for trituration. Total RNA was purified using the RNeasy Mini kit (Qiagen), and microarray analysis was performed by Core Biotech. Purified RNA was used to generate cDNA using the GeneChip Poly-A RNA control kit and the GeneChip One-Cycle cDNA synthesis kit including SuperScript II reverse transcriptase and a T7-(dT)24 primer (Affymetrix). Synthesized cRNA was biotinylated using the GeneChip IVT labeling kit (Affymetrix). Labeled cRNA was purified and chemically fragmented at 94°C for 35 min using the GeneChip Sample Cleanup Module (Affymetrix), and the labeled, fragmented cRNA was hybridized to a GeneChip (*Arabidopsis* ATH1 genome array; Affymetrix) at 45°C for 16 h, according to the manufacturer's instructions. The hybridized probe array was stained and washed with the GeneChip hybridization, wash, and stain kit using a Fluidics Station 450 (Affymetrix).

GeneChip hybridization data were normalized using the MAS5 (Affymetrix Microarray Suite User Guide, version 5; Affymetrix). Hybridization data were analyzed using GenPlex v3.0 software (ISTECH) to identify genes that showed differential expression between *ppi2* and wild-type plants. Fold change and Welch *t* test were applied to select the differentially expressed genes: the fold change threshold was twofold with a significance level of  $P < 0.05$ . Furthermore, the probe sets with "A" or "M

calls" in the sample data were removed to filter false positives. Each probe set of Affymetrix GeneChip data has a detection call: P, "present call" considered as good quality; M, "marginal call" of intermediate quality; A, "absent call" of relatively low reliability.

### RT-PCR Analysis of Transcripts

For RT-PCR analysis, total RNA was isolated from 7-d-old seedlings grown on MS plates using an RNeasy mini kit (Qiagen). Reverse transcription was performed with 2  $\mu$ g of total RNA using SuperScript II (Invitrogen) at 42°C for 50 min, followed by heat inactivation of the reverse transcriptase at 70°C for 15 min using random primers mixed with oligo (dT) primer. PCR was performed using Ex Taq polymerase (Takara) at 94°C for 30 s, 50°C for 30 s, and 72°C for 30 s for 25 cycles using gene-specific primers (see Supplemental Table 1 online). PCR products were visualized by ethidium bromide staining.

### Plasmid Construction

Hsc70-4 cDNA was isolated by PCR amplification using 70-4f and 70-4r primers. The PCR products of *Hsc70-4* were ligated to a T7 tag vector to generate T7:*Hsc70-4*. To construct MBP:*Hsc70-4*, *Hsc70-4* was ligated to pMAL-C2X (New England Biolabs). To construct MBP:*Hsc70-4N* and MBP:*Hsc70-4C*, the N- and C-terminal fragments of Hsc70-4 were generated by PCR (primers: 70-4N-f and 70-4N-r for Hsc70-4N, and 70-4C-f and 70-4C-r for Hsc70-4C) and ligated to pMAL-C2X. The GFP-fused reporter proteins were described previously (Lee et al., 2006, 2008).

*CHIP* was isolated by PCR using CHIP-f and CHIP-r primers, and the *TPR* construct was generated using CHIP-f and TPR-r primers. For T7 epitope tagging, 840-bp *CHIP* and 410-bp *TPR* domain fragments were inserted into a T7 tagging vector. To construct *His:CHIP*, *CHIP* cDNA was isolated from T7:*CHIP* by digesting with *EcoRI* and *XhoI* and ligated into the pcDNA3.1/mys-His vector. The presequence of the F1-ATPase  $\gamma$  subunit (N-terminal 77 amino acid residues, F1) was fused to GFP (Jin et al., 2003). To generate F1m, 10 Ala residues were introduced at amino acids 45 to 50 and 55 to 60 by PCR using primers F1m-1-f, F1m-1-r3, F1m-2-f, and F1m-2-r. To generate RA-tp:GFP, RA-tp was amplified using the specific primers RA-f and RA-r. The 240-bp amplified PCR fragment (80 amino acids) was fused to the N terminus of GFP.

### Screening of T-DNA Insertion Mutants

T-DNA insertion mutants of *Hsc70-1*(Salk\_135531) and *Hsc70-2* (Salk\_087844) were isolated from SALK T-DNA insertion lines obtained from the ABRC. The T-DNA insertions were confirmed by PCR using the T-DNA left border primer and the gene-specific primers LP and RP, as described previously (Alonso et al., 2003).

### Generation of Transgenic Plants Harboring RNAi(*Hsc70-4*) and p*Hsc70-4p*:GUS

To generate transgenic plants harboring the *Hsc70-4* RNAi construct, DNA fragments were amplified from *Hsc70-4* cDNA using the following primers: sense fragment, 70-4X and 70-4K; antisense fragment, 70-4B and 70-4C (see Supplemental Table 1 online). The sense and antisense fragments were ligated to the binary vector pART27 (Wesley et al., 2001). The RNAi vector *pART-Hsc70-4* was introduced into *Agrobacterium tumefaciens*. To generate transgenic plants expressing GUS under the *Hsc70-4* promoter, the 2-kb 5' upstream fragment of the *Hsc70-4* promoter (*Hsc70-4p*) was PCR amplified using p*Hsc70-4f* and p*Hsc70-4r* primers and ligated to a construct of the *GUS* coding region. The cauliflower mosaic virus 35S promoter in pBI121 was replaced by the *Hsc70-4* promoter fragment. Plant transformation was performed with



*hsc70-1* and wild-type plants for RNAi and *pHsc70-4p:GUS* constructs, respectively, using the floral dipping method (Clough and Bent, 1998).

### Transient Expression of Plasmid DNAs

Plasmid DNAs were introduced into protoplasts prepared from the leaf tissues of wild-type plants as described previously (Lee et al., 2006). For chemical treatments, transformed or *ppi2* protoplasts were incubated with MG132 or UCH-L3 (Calbiochem) dissolved in DMSO.

### Protein Gel Blot Analysis of Protein Extracts

Protein extracts were prepared from protoplasts or various tissues as described previously (Jin et al., 2001). Protoplasts were lysed by brief sonication in lysis buffer (10 mM Tris-HCl, pH 7.5, 150 mM NaCl, 2.0 mM EDTA, 0.2 mM PMSF, 1% SDS, 2%  $\beta$ -mercaptoethanol, and a protease inhibitor cocktail) and centrifuged (10,000g at 4°C for 10 min) to remove debris. Protein extracts were prepared from wild-type, *ppi2*, and RNAi transgenic plants.

For protein gel blot analysis, proteins were separated using 10 or 15% SDS-polyacrylamide gels. Protein blots were incubated with the appropriate primary antibodies and then developed with an ECL kit (Amersham Pharmacia Biotech). Anti-ubiquitin (Calbiochem), anti-GFP (Clontech), anti-T7 (Norvagen), anti-HA (Roche), anti-Lhcb4 (Agriser), anti-MBP (Clontech), anti-actin (MP Biomedicals), and anti-His (Qiagen) antibodies were used. Images of immunoblots and band intensities were obtained using an LAS3000 image capture system (Fujifilm).

### Immunoprecipitation

To pre-clear samples, protein extracts (100  $\mu$ g of total protein) in immunoprecipitation buffer (150 mM NaCl, 10 mM Tris-HCl, pH 7.4, 1 mM EDTA, 1 mM EGTA, 0.2 mM PMSF, and 1% Triton X-100) were incubated with protein A-Sepharose beads (CL-4B; Amersham) for 30 min and centrifuged at 10,000g for 5 min at 4°C. Primary antibody (2 to 5  $\mu$ g) was then added to the supernatant and incubated for 3 h at 4°C, followed by incubation with protein A-Sepharose beads for 1 h at 4°C. The pellet was washed three times with immunoprecipitation buffer and subjected to immunoblot analyses with the appropriate antibodies.

### Protein Pull-Down Experiments

Recombinant MBP:Hsc70-4 was expressed in *Escherichia coli* and purified using amylose resin (New England Biolabs) according to the manufacturer's protocol. Four peptides covering the RbcS transit peptide were chemically synthesized (Anygen) and immobilized on Sepharose beads (Affigel 10). Sepharose beads with attached peptides were equilibrated with binding buffer (0.1 M MOPS, pH 7.5) and incubated with MBP:Hsc70-4 in pull-down buffer (40 mM HEPES-KOH, pH 7.5, 10 mM KCl, 3 mM MgCl<sub>2</sub>, 0.4 M sucrose, 1 mM EDTA, 1 mM EGTA, 1 mM DTT, and 0.2% Triton X-100). The beads were precipitated at 7000g for 5 min, washed three times with protein pull-down buffer, and analyzed by protein gel blotting using anti-MBP.

### Light and Electron Microscopy

We selected heterozygous RNAi lines by growth on kanamycin (50 mg/L). Seeds obtained from heterozygous RNAi lines (56 and 61) were planted to obtain embryos. Whole-mount preparations of ovules and plastic sections for light microscopy analysis were prepared and analyzed as described (Mayer et al., 1993). Staging of mutant embryos was approximate and based on the stages of wild-type siblings from the same siliques.

For electron microscopy analyses, ovules were subjected to cryofixation by high-pressure freezing (HPM 010; Bal-Tec) and then freeze-substituted in acetone containing 2.5% osmium tetroxide (60 h at -90°C, 8 h at -60°C, 8 h at -35°C, and 1 h at 0°C). This was followed by washing with acetone and embedding in epoxy resin. Ultrathin sections were stained with uranyl acetate and lead citrate.

### Phylogenetic Analysis

*Arabidopsis* Hsp70 homologs together with one rice (*Oryza sativa*) and three human Hsp70s were aligned using ClustalX at the default setting for multiple alignments (Thompson et al., 1997). This alignment was used to construct a neighbor-joining tree by scoring the number of amino acid differences (pairwise distance) and 1000 replicated bootstrap analyses using Molecular Evolutionary Genetics Analysis version 2 (MEGA2) software. Scale bar indicates a difference of 50 amino acids.

### Accession Numbers

Sequence data from this article can be found in the Arabidopsis Genome Initiative or GenBank/EMBL databases under the following accession numbers: *Lhcb4*, At5g01530; *Hsc70-1*, At5g02490; *Hsc70-2*, At5g02500; *Hsc70-3*, At3g09440; *Hsc70-4*, At3g12580; *Hsc70-5*, At1g16030; *BiP-1*, At5g28540; *mtHsp70-1*, At4g37910; *mtHsp70-2*, At5g09590; *cpHsp70-1*, At4g24280; *cpHsp70-2*, At5g49910; *Hsp70-A*, At1g79920; *Hsp70-B*, At1g79930; *Hsp70-C*, At1g11660; *CHIP*, At3g07370; *HSF A2*, At2g26150; *RPN1*, At2g20580; *RPN5B*, At1g09100; *RPN10*, At4g38630; *TOC159*, At4g02510; *TOC75*, At3g46740; *TOC33*, At1g02280; *TOC34*, At5g05000; and *TIC110*, At1g06950.

### Supplemental Data

The following materials are available in the online version of this article.

**Supplemental Figure 1.** Generation of the Anti-Lhcb4 Antibody.

**Supplemental Figure 2.** Phylogenetic Analysis of *Arabidopsis* Hsp70 Homologs.

**Supplemental Figure 3.** Generation of an Anti-Hsc70-4 Antibody.

**Supplemental Figure 4.** Schematic Representation of the Constructs Used in This Study.

**Supplemental Figure 5.** Hsc70-4 Is Involved in the Induction of a Subset of Genes Induced by Inefficiently Imported Precursors.

**Supplemental Figure 6.** Analysis of Transcript Levels in Protoplasts.

**Supplemental Figure 7.** In Vivo Targeting of GFP Reporters Fused to a Serial Overlapping 20-Amino Acid Segment of RbcS-tp in Protoplasts.

**Supplemental Figure 8.** Proteins and Peptides Used in Hsc70-4 and RbcS-tp Binding Experiments.

**Supplemental Figure 9.** Screening and Phenotype of T-DNA Insertion Mutants of *Hsc70-1* and *Hsc70-2*.

**Supplemental Figure 10.** RT-PCR Analysis of 13 Hsp70 Homologs in RNAi Plants.

**Supplemental Figure 11.** Homozygotes of RNAi Plants Display the Developmental Defects.

**Supplemental Figure 12.** *Hsc70-4* Exhibits a Differential Expression Pattern with Strong Expression in Embryos.

**Supplemental Figure 13.** RNAi Plants Contain High Levels of ROS.

**Supplemental Table 1.** Primer Sequences Used in This Study.

**Supplemental Data Set 1.** Sequence Alignment of *Arabidopsis* Hsp70 Homologs.

## ACKNOWLEDGMENTS

We thank Hong Zhang (Texas Tech University) for anti-CHIP antibody. *Arabidopsis* T-DNA insertion mutants were obtained from the ABRC. This study was supported by grants from the Creative Research Initiatives Program and the World Class University project of the Ministry of Science and Technology (Korea), and the Systems Biodynamics National Core Research Center, Technology Development Program for Agriculture and Forestry (107103-3).

Received September 21, 2009; revised November 18, 2009; accepted December 5, 2009; published December 22, 2009.

## REFERENCES

- Agne, B., and Kessler, F.** (2009). Protein transport in organelles: The Toc complex way of preprotein import. *FEBS J.* **276**: 1156–1165.
- Alonso, J.M., et al.** (2003). Genome-wide insertional mutagenesis of *Arabidopsis thaliana*. *Science* **301**: 653–657.
- Apel, K., and Hirt, H.** (2004). Reactive oxygen species: Metabolism, oxidative stress, and signal transduction. *Annu. Rev. Plant Biol.* **55**: 373–399.
- Baldwin, D., Crane, V., and Rice, D.** (1999). A comparison of gel-based, nylon filter and microarray techniques to detect differential RNA expression in plants. *Curr. Opin. Plant Biol.* **2**: 96–103.
- Ballinger, C.A., Connell, P., Wu, Y., Hu, Z., Thompson, L.J., Yin, L.Y., and Patterson, C.** (1999). Identification of CHIP, a novel tetratricopeptide repeat-containing protein that interacts with heat shock proteins and negatively regulates chaperone functions. *Mol. Cell Biol.* **19**: 4535–4545.
- Bauer, J., Chen, K., Hiltbunner, A., Wehri, E., Eugster, M., Schnell, D., and Kessler, F.** (2000). The major protein import receptor of plastids is essential for chloroplast biogenesis. *Nature* **403**: 203–207.
- Brlkjacic, J., Zhao, Q., and Meier, I.** (2009). WPP-domain proteins mimic the activity of the HSC70-1 chaperone in preventing mistargeting of RanGAP1-anchoring protein WIT1. *Plant Physiol.* **151**: 142–154.
- Bruce, B.D.** (2001). The paradox of plastid transit peptides: conservation of function despite divergence in primary structure. *Biochim. Biophys. Acta* **1541**: 2–21.
- Bukau, B., and Horwich, A.L.** (1998). The Hsp70 and Hsp60 chaperone machines. *Cell* **92**: 351–366.
- Bukau, B., Weissman, J., and Horwich, A.** (2006). Molecular chaperones and protein quality control. *Cell* **125**: 443–451.
- Cazalé, A.C., Clément, M., Chiarenza, S., Roncato, M.A., Pochon, N., Creff, A., Marin, E., Leonhardt, N., and Noël, L.D.** (2009). Altered expression of cytosolic/nuclear HSC70-1 molecular chaperone affects development and abiotic stress tolerance in *Arabidopsis thaliana*. *J. Exp. Bot.* **60**: 2653–2664.
- Cho, D., Shin, D., Jeon, B.W., and Kwak, J.M.** (2009). ROS-mediated ABA signaling. *J. Plant Biol.* **52**: 102–113.
- Clough, S.J., and Bent, A.F.** (1998). Floral dip: A simplified method for *Agrobacterium*-mediated transformation of *Arabidopsis thaliana*. *Plant J.* **16**: 735–743.
- Connell, P., Ballinger, C.A., Jiang, J., Wu, Y., Thompson, L.J., Höhfeld, J., and Patterson, C.** (2001). The co-chaperone CHIP regulates protein triage decisions mediated by heat-shock proteins. *Nat. Cell Biol.* **3**: 93–96.
- Cyr, D.M., Höhfeld, J., and Patterson, C.** (2002). Protein quality control: U-box-containing E3 ubiquitin ligases join the fold. *Trends Biochem. Sci.* **27**: 368–375.
- Dickson, R., Weiss, C., Howard, R.J., Aldrick, S.P., Ellis, R.J., Lorimer, G., Azem, A., and Viitanen, P.V.** (2000). Reconstitution of higher plant chloroplast chaperonin 60 tetradecamers active in protein folding. *J. Biol. Chem.* **275**: 11829–11835.
- Esser, C., Alberti, S., and Hohfeld, J.** (2004). Cooperation of molecular chaperones with the ubiquitin/proteasome system. *Biochim. Biophys. Acta* **1695**: 171–188.
- Fernández, A.P., and Strand, A.** (2008). Retrograde signaling and plant stress: Plastid signals initiate cellular stress responses. *Curr. Opin. Plant Biol.* **11**: 509–513.
- Hampton, R.Y.** (2000). ER stress response: Getting the UPR hand on misfolded proteins. *Curr. Biol.* **10**: R518–R521.
- Hartl, F.U., and Hayer-Hartl, M.** (2002). Molecular chaperones in the cytosol: from nascent chain to folded protein. *Science* **295**: 1852–1858.
- Hatakeyama, S., and Nakayama, K.I.** (2003). Ubiquitylation as a quality control system for intracellular proteins. *J. Biochem.* **134**: 1–8.
- Hershko, A., Ciechanover, A., and Varshavsky, A.** (2000). The ubiquitin system. *Nat. Med.* **6**: 1073–1081.
- Ivey, R.A., and Bruce, B.D.** (2000). In vivo and in vitro interaction of DnaK and a chloroplast transit peptide. *Cell Stress Chaperones* **5**: 62–71.
- Ivey, R.A., Subramanian, C., and Bruce, B.D.** (2000). Identification of a Hsp70 recognition domain within the rubisco small subunit transit peptide. *Plant Physiol.* **122**: 1289–1299.
- Jarvis, P.** (2008). Targeting of nucleus-encoded proteins to chloroplasts in plants. *New Phytol.* **179**: 257–285.
- Jarvis, P., and Soll, J.** (2002). Toc, tic, and chloroplast protein import. *Biochim. Biophys. Acta* **1590**: 177–189.
- Jiang, J., Ballinger, C.A., Wu, Y., Dai, Q., Cry, D.M., Höhfeld, J., and Patterson, C.** (2001). CHIP is a U-box-dependent E3 ubiquitin ligase: identification of Hsc70 as a target for ubiquitylation. *J. Biol. Chem.* **276**: 42938–42944.
- Jin, J.B., Bae, H., Kim, S.J., Jin, Y.H., Goh, C.H., Kim, D.H., Lee, Y.J., Tse, Y.C., Jiang, L., and Hwang, I.** (2003). The *Arabidopsis* dynamin-like proteins ADL1C and ADL1E play a critical role in mitochondrial morphogenesis. *Plant Cell* **15**: 2357–2369.
- Jin, J.B., Kim, Y.A., Kim, S.J., Lee, S.H., Kim, D.H., Cheong, G.W., and Hwang, I.** (2001). A new dynamin-like protein, ADL6, is involved in trafficking from the trans-Golgi network to the central vacuole in *Arabidopsis*. *Plant Cell* **13**: 1511–1526.
- Kabashi, E., and Durham, H.D.** (2006). Failure of protein quality control in amyotrophic lateral sclerosis. *Biochim. Biophys. Acta* **1762**: 1038–1050.
- Keegstra, K., and Froehlich, J.E.** (1999). Protein import into chloroplasts. *Curr. Opin. Plant Biol.* **2**: 471–476.
- Kim, R., Emi, M., Tanabe, K., and Murakami, S.** (2006). Role of the unfolded protein response in cell death. *Apoptosis* **11**: 5–13.
- Klimmek, F., Sjödin, A., Noutsos, C., Leister, D., and Jansson, S.** (2006). Abundantly and rarely expressed Lhc protein genes exhibit distinct regulation patterns in plants. *Plant Physiol.* **140**: 793–804.
- Ko, K., Bornemisza, O., Kourtz, L., Ko, Z.W., Plaxton, W.C., and Cashmore, A.R.** (1992). Isolation and characterization of a cDNA clone encoding a cognate 70-kDa heat shock protein of the chloroplast envelope. *J. Biol. Chem.* **267**: 2986–2993.
- Koumoto, Y., Shimada, T., Kondo, M., Hara-Nishimura, I., and Nishimura, M.** (2001). Chloroplasts have a novel Cpn10 in addition to Cpn20 as co-chaperonins in *Arabidopsis thaliana*. *J. Biol. Chem.* **276**: 29688–29694.
- Kourtz, L., and Ko, K.** (1997). The early stage of chloroplast protein import involves Com70. *J. Biol. Chem.* **272**: 2808–2813.

- Król, M., Spangfort, M.D., Huner, N.P., Oquist, G., Gustafsson, P., and Jasson, S. (1995). Chlorophyll a/b-binding proteins, pigment conversions, and early light-induced proteins in a chlorophyll b-less barley mutant. *Plant Physiol.* **107**: 873–883.
- Kubis, S., Baldwin, A., Patel, R., Razzaq, A., Dupree, P., Lilley, K., Kurth, J., Leister, D., and Jarvis, P. (2003). The *Arabidopsis* ppi1 mutant is specifically defective in the expression, chloroplast import, and accumulation of photosynthetic proteins. *Plant Cell* **15**: 1859–1871.
- Kubis, S., Patel, R., Combe, J., Bédard, J., Kovacheva, S., Lilley, K., Biehl, A., Leister, D., Rios, G., Koncz, C., and Jarvis, P. (2004). Functional specialization amongst the *Arabidopsis* Toc159 family of chloroplast protein import receptors. *Plant Cell* **16**: 2059–2077.
- Lee, D.H., and Goldberg, A.L. (1998). Proteasome inhibitors: valuable new tools for cell biologists. *Trends Cell Biol.* **8**: 397–403.
- Lee, D.W., Kim, J.K., Lee, S., Choi, S., Kim, S., and Hwang, I. (2008). *Arabidopsis* nuclear-encoded plastid transit peptides contain multiple sequence subgroups with distinctive chloroplast-targeting sequence motifs. *Plant Cell* **20**: 1603–1622.
- Lee, D.W., Lee, S., Lee, G.J., Lee, K.H., Kim, S., Cheong, G.W., and Hwang, I. (2006). Functional characterization of sequence motifs in the transit peptide of *Arabidopsis* small subunit of rubisco. *Plant Physiol.* **140**: 466–483.
- Lee, K.H., Kim, D.H., Lee, S.W., Kim, Z.H., and Hwang, I. (2003). In vivo import experiments in protoplasts reveal the importance of the overall context but not specific amino acid residues of the transit peptide during import into chloroplasts. *Mol. Cells* **14**: 388–397.
- Lin, B.L., Wang, J.S., Liu, H.C., Chen, R.W., Meyer, Y., Barakat, A., and Delseny, M. (2001). Genomic analysis of the Hsp70 superfamily in *Arabidopsis thaliana*. *Cell Stress Chaperones* **6**: 201–208.
- Liu, Y., Lashuel, H.A., Choi, S., Xing, X., Case, A., Ni, J., Yeh, L.A., Cuny, G.D., Stein, R.L., and Lansbury, P.T. (2003). Discovery of inhibitors that elucidate the role of UCH-L1 activity in the H1299 lung cancer cell line. *Chem. Biol.* **10**: 837–846.
- Luo, J., Shen, G., Yan, J., He, C., and Zhang, H. (2006). AtCHIP functions as an E3 ubiquitin ligase of protein phosphatase 2A subunits and alters plant response to abscisic acid treatment. *Plant J.* **46**: 649–657.
- Ma, Y., and Hendershot, L.M. (2001). The unfolding tale of the unfolded protein response. *Cell* **107**: 827–830.
- May, T., and Soll, J. (2000). 14-3-3 proteins form a guidance complex with chloroplast precursor proteins in plants. *Plant Cell* **12**: 53–64.
- Mayer, U., Büttner, G., and Jürgens, G. (1993). Apical-basal pattern formation in the *Arabidopsis* embryo: Studies on the role of the *gnom* gene. *Development* **117**: 149–162.
- McDonough, H., and Patterson, C. (2003). CHIP: A link between the chaperone and proteasome systems. *Cell Stress Chaperones* **8**: 303–308.
- Meredith, S.C. (2005). Protein denaturation and aggregation: Cellular responses to denatured and aggregated proteins. *Ann. N. Y. Acad. Sci.* **1066**: 181–221.
- Murata, S., Minami, Y., Minami, M., Chiba, T., and Tanaka, K. (2001). CHIP is a chaperone-dependent E3 ligase that ubiquitylates unfolded protein. *EMBO Rep.* **2**: 1133–1138.
- Nelson, R.F., Glenn, K.A., Miller, V.M., Wen, H., and Paulson, H.L. (2006). A novel route for F-box protein-mediated ubiquitination links CHIP to glycoprotein quality control. *J. Biol. Chem.* **281**: 20242–20251.
- Noël, L.D., Cagna, G., Stuttmann, J., Wirthmüller, L., Betsuyaku, S., Witte, C.P., Bhat, R., Pochon, N., Colby, T., and Parker, J.E. (2007). Interaction between SGT1 and cytosolic/nuclear HSC70 chaperones regulates *Arabidopsis* immune responses. *Plant Cell* **19**: 4061–4076.
- Overmyer, K., Brosché, M., and Kangasjärvi, J. (2003). Reactive oxygen species and hormonal control of cell death. *Trends Plant Sci.* **8**: 335–342.
- Saibil, H.R., and Ranson, N.A. (2002). The chaperonin folding machine. *Trends Biochem. Sci.* **27**: 627–632.
- Schubert, U., Antón, L.C., Gibbs, J., Norbury, C.C., Yewdell, J.W., and Bennink, J.R. (2000). Rapid degradation of a large fraction of newly synthesized proteins by proteasomes. *Nature* **404**: 770–774.
- Shen, G., Adam, Z., and Zhang, H. (2007a). The E3 ligase AtCHIP ubiquitylates FtsH1, a component of the chloroplast FtsH protease, and affects protein degradation in chloroplasts. *Plant J.* **52**: 309–321.
- Shen, G., Yan, J., Pasapula, V., Luo, J., He, C., Clarke, A.K., and Zhang, H. (2007b). The chloroplast protease subunit ClpP4 is a substrate of the E3 ligase AtCHIP and plays an important role in chloroplast function. *Plant J.* **49**: 228–237.
- Smalle, J., and Vierstra, R.D. (2004). The ubiquitin 26S proteasome proteolytic pathway. *Annu. Rev. Plant Biol.* **55**: 555–590.
- Soll, J., and Schleiff, E. (2004). Protein import into chloroplasts. *Nat. Rev. Mol. Cell Biol.* **5**: 198–208.
- Sung, D.Y., and Guy, C.L. (2003). Physiological and molecular assessment of altered expression of Hsc70-1 in *Arabidopsis*. Evidence for pleiotropic consequences. *Plant Physiol.* **132**: 979–987.
- Sung, D.Y., Vierling, E., and Guy, C.L. (2001). Comprehensive expression profile analysis of the *Arabidopsis* Hsp70 gene family. *Plant Physiol.* **126**: 789–800.
- Thompson, J.D., Gibson, T.J., Plewniak, F., Jeanmougin, F., and Higgins, D.G. (1997). The ClustalX windows interface: flexible strategies for multiple sequence alignment aided by quality analysis tools. *Nucleic Acids Res.* **24**: 4876–4882.
- Wesley, S.V., Helliwell, C.A., Smith, N.A., Wang, M.B., Rouse, D.T., Liu, Q., Gooding, P.S., Singh, S.P., Abbott, D., Stoutjesdijk, P.A., Robinson, S.P., Gleave, A.P., Green, A.G., and Waterhouse, P.M. (2001). Construct design for efficient, effective and high-throughput gene silencing in plants. *Plant J.* **27**: 581–590.
- Wickner, S., Maurizi, M.R., and Gottesman, S. (1999). Posttranslational quality control: Folding, refolding, and degrading proteins. *Science* **286**: 1888–1893.